

# **STUDY OF TALL BUILDINGS FOR WIND-INDUCED LOAD REDUCTION BY CORNER MODIFICATION AND PROVIDING LARGE OPENINGS**

**A Dissertation Submitted  
In Partial Fulfilment of the Requirements for the  
Degree of  
MASTER OF TECHNOLOGY**

**in  
Structural Engineering  
by**

**Madan Meena**

**(2K22/STE/06)**

**Under the Supervision of  
Dr. Ritu Raj  
Assistant Professor  
Delhi Technological University**



**Department of Civil Engineering  
DELHI TECHNOLOGICAL UNIVERSITY  
(Formerly Delhi College of Engineering)  
Shahbad Daultpur, Main Bawana Road, Delhi-110042, India**

**May, 2024**



# DELHI TECHNOLOGICAL UNIVERSITY

(Formerly Delhi College of Engineering)

Shahbad Daultpur, Main Bawana Road, Delhi-42

## CANDIDATE'S DECLARATION

I **Madan Meena** hereby certify that the work which is being presented in the thesis entitled **Study of tall buildings for wind-induced load reduction by corner modification and providing large openings** in partial fulfilment of the requirements for the award of the Degree of Master in Technology, submitted in the Department of **Civil Engineering**, Delhi Technological University is an authentic record of my own work carried out during the period from **August,2023** to **May,2024** under the supervision of **Dr. Ritu Raj**

The matter presented in the thesis has not been submitted by me for the award of any other degree of this or any other Institute.

A handwritten signature in blue ink that reads "madan" with two horizontal lines underneath.

**Candidate's Signature**

This is to certify that the student has incorporated all the corrections suggested by the examiners in the thesis and the statement made by the candidate is correct to the best of our knowledge.

A handwritten signature in blue ink that appears to read "Ritu Raj" with a stylized flourish.

**Signature of Supervisor**

**Signature of External Examiner**



# DELHI TECHNOLOGICAL UNIVERSITY

(Formerly Delhi College of Engineering)

Shahbad Daultpur, Main Bawana Road, Delhi-42

## CERTIFICATE BY THE SUPERVISOR

Certified that **Madan Meena** (2K22/STE/06) has carried out his search work presented in this thesis entitled “Study of tall buildings for wind-induced load reduction by corner modification and providing large openings”, for the award of **Master of Technology** from Department of Civil Engineering, Delhi Technological University, Delhi, under my supervision. The thesis embodies results of original work, and studies are carried out by the student himself and the contents of the thesis do not form the basis for the award of any other degree to the candidate or to anybody else from this or any other University/Institution.

A handwritten signature in blue ink, appearing to read "Ritu Raj", is placed within a light blue rectangular box.

Signature

Dr. Ritu Raj  
Assistant Professor  
Delhi Technological University

Date

## ABSTRACT

As urban populations continue to grow, cities are experiencing a significant shortage of space for both residential and commercial developments. This spatial constraint has driven the demand for taller buildings, which, while efficient in terms of space utilization, are particularly susceptible to the effects of wind-induced loads and motions. Therefore, mitigating these wind effects in tall buildings is crucial for their structural integrity and safety.

This study focuses on analyzing wind pressure on tall buildings with a square cross-section, particularly examining the combined impact of corner modifications and the inclusion of large openings. The analysis is conducted using Computational Fluid Dynamics (CFD) in ANSYS Workbench, applied to models scaled at 1:100. Specifically, the corners of the buildings are altered to include recessed corners and chamfered corners, while the large openings are varied to cover 10%, 20%, and 30% of the building's frontal area.

The aim is to determine how these design modifications influence the aerodynamic mean pressure coefficient ( $C_p$ ) and the pressure distribution across different faces of the building models. By comparing these results, the study seeks to identify the configuration that minimizes wind load on the structure.

In essence, the research explores innovative structural modifications that can effectively reduce wind-induced stress on high-rise buildings. Recessed and chamfered corners are two structural adjustments examined for their potential to disrupt wind flow and reduce pressure on the building's surface. Additionally, varying the size of large frontal openings is analyzed to understand how these gaps can alleviate wind pressure by allowing airflow through the building rather than around it.

The findings from this CFD analysis are critical as they provide insights into optimizing the design of tall buildings to withstand wind forces. By identifying the corner modifications and opening sizes that result in the lowest wind loads, architects and engineers can enhance the resilience and stability of skyscrapers in urban environments. This research contributes to the broader field of structural engineering by offering practical solutions to the challenges posed by wind loads on tall buildings, thereby supporting the development of safer and more sustainable urban landscapes.

## ACKNOWLEDGEMENT

Completing the research thesis, "**Study of tall buildings for wind-induced load reduction by corner modification and providing large openings**," has been full of growth opportunities, obstacles, and vital assistance. Upon reflection of this endeavours, I am incredibly appreciative of everyone who helped make it happen.

First and foremost, I want to express my heartfelt gratitude to my thesis supervisor, **Dr. Ritu Raj**, whose guidance, experience, and support have helped shape this research. Their guidance and encouragement have been invaluable throughout the duration of this project.

I am also thankful to **Deepak Sharma**, PhD scholar in DTU for their insightful feedback, constructive criticism, and scholarly guidance. Their expertise has significantly enriched the quality and depth of this thesis.

I am grateful to my institute, **Delhi Technological University**, dept. of Civil Engineering, for providing the necessary resources, facilities, and academic environment conducive to research. The institutional support has been vital in facilitating the completion of this study.

I would like to acknowledge the assistance and cooperation of my colleagues, **Subodh Bende, P. Pavan Kumar & Bimal Sharma** whose discussions, feedback, and encouragement have been invaluable throughout this journey. Their camaraderie and support have made this endeavour all the more rewarding.

Lastly, I am deeply grateful to my family for their unwavering support, patience, and understanding during this academic pursuit. Their love and encouragement have been a constant source of strength and motivation.

In conclusion, I extend my sincere appreciation to all individuals and entities who have contributed to this research thesis, directly or indirectly. Your support has been instrumental in its completion.

Thank you

(Madan Meena)

## **TABLE OF CONTENTS**

<b>CANDIDATE’S DECLARATION .....</b>	<b>i</b>
<b>CERTIFICATE .....</b>	<b>ii</b>
<b>ABSTRACT .....</b>	<b>iii</b>
<b>ACKNOWLEDGEMENT .....</b>	<b>iv</b>
<b>TABLE OF CONTENTS .....</b>	<b>v</b>
<b>LIST OF TABLES .....</b>	<b>viii</b>
<b>LIST OF FIGURES.....</b>	<b>ix</b>
<b>LIST OF SYMBOLS.....</b>	<b>..xi</b>
<b>LIST OF ABBREVIATIONS.....</b>	<b>xiii</b>

## **CHAPTER 1 INTRODUCTION**

<b>1.1 General.....</b>	<b>1</b>
<b>1.2 Wind Load on Tall Buildings.....</b>	<b>2</b>
<b>1.3 Computational Fluid Dynamics (CFD).....</b>	<b>4</b>
<b>1.4 Objectives and scope of the study.....</b>	<b>6</b>
<b>1.5 Outline of thesis.....</b>	<b>7</b>

## **CHAPTER 2 Literature Review**

<b>2.1 General.....</b>	<b>9</b>
<b>2.2 Indian Standards (IS 875:part-3:2015) .....</b>	<b>9</b>
<b>2.3 Literature Review.....</b>	<b>12</b>
<b>2.4 Research Gap.....</b>	<b>22</b>

## **CHAPTER 3 METHODOLOGY**

<b>3.1</b>	<b>General.....</b>	<b>23</b>
<b>3.2</b>	<b>Numerical Simulations.....</b>	<b>23</b>
<b>3.3</b>	<b>Computational Fluid Dynamics (CFD).....</b>	<b>23</b>
<b>3.4</b>	<b>Modelling.....</b>	<b>24</b>
<b>3.5</b>	<b>Model Details.....</b>	<b>26</b>
<b>3.6</b>	<b>Boundary Conditions.....</b>	<b>28</b>
<b>3.7</b>	<b>Meshing.....</b>	<b>29</b>
<b>3.8</b>	<b>Validation.....</b>	<b>31</b>

## **CHAPTER 4 RESULTS AND DISCUSSION**

<b>4.1</b>	<b>General.....</b>	<b>32</b>
<b>4.2</b>	<b>Pressure contours.....</b>	<b>32</b>
<b>4.3</b>	<b>Velocity streamlines.....</b>	<b>37</b>
<b>4.4</b>	<b>Coefficient of Pressure (<math>C_p</math>).....</b>	<b>39</b>
<b>4.5</b>	<b>Drag Force Coefficients (<math>C_{fx}</math> &amp; <math>C_{fy}</math>) .....</b>	<b>43</b>

## **CHAPTER 5 CONCLUSION**

<b>5.1</b>	<b>Summary.....</b>	<b>46</b>
<b>5.2</b>	<b>Conclusion.....</b>	<b>46</b>

<b>REFERENCES.....</b>	<b>47</b>
------------------------	-----------

<b>SCOPUS INDEXED CONFERENCE CERTIFICATE.....</b>	<b>51</b>
---	-----------

## **List of Tables**

<b>Table 2.1 Wind Pressure Coefficients on Rectangular Clad Building .....</b>	<b>10</b>
<b>Table 4. 1 Coefficient of pressure (<math>C_p</math>) for Model A for different % of Opening conditions .....</b>	<b>40</b>
<b>Table 4. 2 Coefficient of pressure (<math>C_p</math>) for Model B for different % of Opening conditions .....</b>	<b>41</b>
<b>Table 4. 3 Coefficient of pressure (<math>C_p</math>) for Model C for different % of Opening conditions .....</b>	<b>41</b>



## List of Figures

<b>Fig.1.1</b> Examples of some tall Buildings (Source: Google Images).....	2
<b>Fig. 2. 1</b> Force coefficient for rectangular clad buildings in uniform flow.....	11
<b>Fig. 3. 1</b> Plan View of Models with various Corner Modifications.....	26
<b>Fig. 3. 2</b> Isometric view of Model A,B and C .....	27
<b>Fig. 3. 3</b> Domain used in CFD Simulation .....	28
<b>Fig. 3. 4</b> Different types of Meshing(a) Building Meshing (b) Domain Meshing .....	30
<b>Fig. 4. 1</b> Pressure contours at different percentage of openings of Model A.....	34
<b>Fig. 4. 2</b> Pressure contours at different percentage of openings of Model B.....	35
<b>Fig. 4. 3</b> Pressure contours at different percentage of openings of Model C.....	36
<b>Fig. 4. 4</b> Streamlines for Model A for different opening conditions.....	37
<b>Fig. 4. 5</b> Streamlines for Model B for different opening conditions.....	38
<b>Fig. 4. 6</b> Streamlines for Model C for different opening conditions.....	38
<b>Fig. 4. 7</b> Coefficient of pressure ( $C_p$ ) for Model A for different % of Opening conditions..	42
<b>Fig. 4. 8</b> Coefficient of pressure ( $C_p$ ) for Model A for different % of Opening conditions..	42
<b>Fig. 4. 9</b> Coefficient of pressure ( $C_p$ ) for Model A for different % of Opening conditions...	42
<b>Fig. 4. 10</b> Coefficient of Drag in X-direction ( $C_{fx}$ ) for $0^\circ$ incidence angle .....	44
<b>Fig. 4. 11</b> Coefficient of Drag in X-direction ( $C_{fx}$ ) for $30^\circ$ incidence angle.....	45

## List of Symbols

$C_p$ - Coefficient of pressure  
 $V_b$ - Basic wind speed  
 $K_1$ -Probability factor  
 $K_2$ - Terrain, height and structure size factor  
 $K_3$ - Topography factor  
 $K_4$  - Importance factor for cyclonic region  
 $P_z$  - Wind pressure at height Z  
 $V_z$  - Design wind speed at height Z  
 $K_d$  - Wind directionality factor  
 $K_a$  - Area averaging factor  
 $K_c$  - Combination factor  
 $F$  - Wind force  
 $C_{pe}$  - External pressure coefficient  
 $C_{pi}$  - Internal pressure coefficient  
 $A$  - Effective area of structure  
 $P_d$  - Design wind pressure  
 $F$  - Wind force  
 $C_f$  - Force coefficient  
 $A$  - Effective area of structure  
 $P_d$  - Design wind pressure  
 $C_{fx}$ - Coefficient of pressure in X direction  
 $C_{fy}$ - Coefficient of pressure in Y direction

## **List of Abbreviations**

**CFD-** Computational Fluid Dynamics

**FEM-** Finite Element Model

# CHAPTER 1

## INTRODUCTION

### 1.1 General

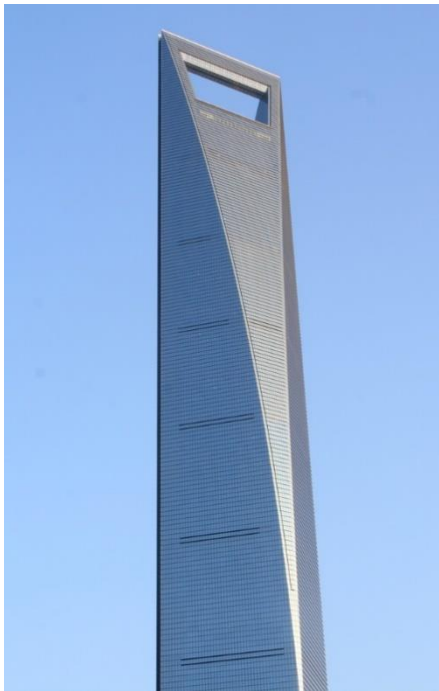
The construction of tall buildings has become essential in modern cities, driven largely by the rapid urbanization and population growth we see today. As more people move to urban areas seeking better economic opportunities, education, and healthcare, cities face a significant challenge: limited space to accommodate everyone. Expanding horizontally often isn't practical due to geographic constraints, existing infrastructure, and environmental concerns. As a result, building upwards with tall structures becomes a smart solution, allowing cities to house more residents and businesses within a confined area.

Tall buildings help address space shortages and boost economic vitality. High-rises can pack a lot of residential units, offices, retail spaces, and other businesses into a single footprint. This mix of functions in one place creates a vibrant urban environment, sparking economic activity and innovation. Additionally, by bringing amenities and services closer together, tall buildings can reduce the need for long commutes, easing traffic congestion and lowering carbon emissions. This approach supports sustainable urban development and improves the overall quality of life for city residents.

Beyond their practical benefits, tall buildings often symbolize progress and modernity, reflecting our aspirations and technological advancements. Iconic skyscrapers can become landmarks, attracting tourists and boosting a city's global profile. They showcase architectural achievements and engineering prowess, highlighting what we can accomplish with modern construction techniques and materials. Moreover, tall

buildings play a crucial role in urban planning and design, shaping the skyline and defining the identity of a city. By incorporating innovative designs and sustainable practices, these structures can set the standard for future developments, promoting resilience and adaptability as cities evolve.

In essence, the need for tall buildings in today's cities stems from the necessity to make the most of limited space, drive economic growth, and embody societal progress. These structures offer practical solutions to the challenges posed by urbanization, enabling cities to accommodate growing populations while fostering sustainable and dynamic communities. As cities continue to grow and change, tall buildings will remain a vital part of their development, helping to create liveable, efficient, and forward-looking urban environments.



0



**Fig.1.1** Examples of some tall Buildings (Source: Google Images)

## **1.2 Wind Load on Tall Buildings**

Understanding and mitigating wind load on tall buildings is paramount to ensuring their structural integrity and the safety of occupants. Tall buildings are particularly vulnerable to the effects of wind due to their height and exposure, making wind load analysis an essential aspect of their design and construction.[1]

Firstly, wind load directly impacts the stability and durability of tall buildings. As wind flows around and against these towering structures, it exerts pressure on their surfaces, generating forces that can induce structural deformation, sway, and even structural failure if not adequately addressed. By accurately assessing wind loads, engineers can design tall buildings to withstand these forces, ensuring their resilience against varying wind speeds and directions.

Moreover, wind load analysis influences architectural and structural decisions during the design phase. Engineers consider factors such as building shape, orientation, and surface features when evaluating wind effects. By optimizing these design parameters, they can minimize wind-induced vibrations, reduce structural stresses, and enhance overall building performance. Additionally, wind load considerations inform the selection of building materials, reinforcing elements, and construction techniques to enhance resilience and safety.

Beyond structural concerns, wind load analysis also impacts the comfort and usability of tall buildings. Excessive wind-induced vibrations or swaying can cause discomfort for occupants, affecting their productivity and well-being. Furthermore, strong winds may pose operational challenges for building systems such as HVAC, elevators, and façade elements. By accounting for wind loads in design, engineers can mitigate these issues, creating a more comfortable and functional environment for occupants.

In densely populated urban areas, tall buildings interact with surrounding structures and the local wind environment, creating complex aerodynamic interactions. Wind load analysis helps anticipate these interactions, enabling engineers to identify potential issues such as wind tunnel effects, vortex shedding, and wind-induced resonance. By understanding these phenomena, designers can implement mitigation measures and optimize building layouts to minimize adverse effects on occupants and neighbouring structures.

In conclusion, the importance of wind load analysis for tall buildings cannot be overstated. By accurately assessing wind effects and integrating appropriate design measures, engineers can ensure the structural integrity, safety, and usability of tall buildings in various wind conditions. This proactive approach not only safeguards lives and property but also contributes to the resilience and sustainability of our built environment.

Wind load reduction can be accomplished by three ways: (i) By providing adequate structural elements and Systems for external damping, (ii) By implementing aerodynamic measures to reduce the impact of wind on the outer structure of a building, or (iii) By integrating the aforementioned approaches to enhance both the structural integrity and aerodynamic efficiency of the building.

The first method involves allocating extra resources, such as enhancing the strength of structural components and implementing damping systems, in order to maintain the original shape of the building.

The second method reduces the cost by decreasing the wind load exerted on the building by aerodynamic measures. In certain scenarios, meeting the necessary strength and serviceability criteria is only achievable when both structural enhancements and aerodynamic improvements are implemented.

Many of the most recently constructed super-tall buildings have incorporated aerodynamic measures into their design, either through localized modifications, such

as adjustments to corners, or through global alterations, such as incorporating large openings throughout the height of the building.

Although reports on vertical aerodynamic treatments shows that it helps in reducing across-wind loads and its responses on tall buildings. Making minor adjustments to the horizontal shape of tall buildings is typically more convenient and feasible for structural designers compared to implementing vertical aerodynamic treatments. Additionally, such horizontal modifications are often more readily accepted by building owners. Indeed, horizontal modifications to building corners have been demonstrated that it effectively reduces wind effects on tall buildings.

### **1.3 Computational Fluid Dynamics (CFD)**

Computational Fluid Dynamics (CFD) is a powerful tool used to simulate and analyse the behaviour of fluid flows, including air, around complex objects like tall buildings. It involves using mathematical algorithms to solve the governing equations of fluid motion, such as the Navier-Stokes equations, on a computational grid that represents the physical domain. By dividing the fluid domain into discrete cells and solving equations for each cell, CFD enables engineers to predict how air flows, pressure distributions, and other fluid properties vary across different regions.

In the context of wind load analysis for tall buildings, CFD plays a crucial role in assessing the aerodynamic effects of wind on building surfaces. Engineers use CFD simulations to model the interaction between wind and tall building geometries, considering factors such as building shape, orientation, surface roughness, and nearby structures. By inputting relevant parameters and boundary conditions into the CFD software, engineers can simulate wind flow patterns around the building and predict the distribution of wind pressures on its surfaces.



CFD provides detailed insights into how wind interacts with different parts of the building, including corners, edges, and openings, influencing wind-induced loads and structural responses. Engineers can analyse factors such as wind-induced vibrations, vortex shedding, and wind pressures on critical structural elements to assess the building's overall stability and performance under varying wind conditions. Additionally, CFD allows for the evaluation of different design strategies and mitigation measures to optimize the building's aerodynamic performance and reduce wind-induced effects.

Overall, CFD facilitates a comprehensive understanding of the complex fluid dynamics involved in wind load analysis for tall buildings. By leveraging CFD simulations, engineers can accurately predict wind-induced loads and their effects on building structures, enabling informed design decisions and enhancing the safety and resilience of tall buildings in high-speed wind environments.

#### **1.4 Objectives and scope of the study**

The main objective of this research is to **Study of tall buildings for wind-induced load reduction by corner modification and providing large openings**. In this study, the research has been conducted on horizontal and vertical aerodynamic treatments to mitigate wind effects on tall buildings, there remains a lack of research on the combined effects of corner modifications and large openings along the height of buildings for reducing wind loads on tall structures. Given the widespread use of square sections in tall building design for their simplicity and aesthetic appeal, a square section model is selected as the benchmark for this study. The different corner modification (Recessed and Chamfered Corners) with a 10% cut rate, combined with openings of 10%, 20%, and 30% along the height of the building, are considered for reduction of wind loads on tall buildings through computational fluid dynamics (CFD) simulations in ANSYS WORKBENCH.

The comprehensive analysis and comparison of various corner modifications and large openings on wind loads and structural integrity in tall buildings involve a meticulous examination of how different design features impact the behaviour of wind around the building. This process entails studying factors such as the shape and size of recessed or chamfered corners, as well as the percentage of the building's frontal area occupied by large openings. In this study we need to consider how these modifications affect the flow of air around the building, including how they alter wind pressure distribution, turbulence, and potential structural vulnerabilities. By conducting thorough analyses and comparisons, we can identify which design configurations are most effective in reducing wind loads and enhancing the structural resilience of tall buildings.

Measuring and comparing various parameters such as wind pressure distributions, viscosity coefficients, turbulence viscosity, drag force coefficients, and lift force coefficients for different corner designs and opening configurations provide crucial insights into how each design element influences wind behaviour. Wind pressure distributions indicate how pressure varies across the building's surfaces, which is essential for understanding where structural stresses are concentrated. Viscosity coefficients and turbulence viscosity help characterize the viscosity of air and how it affects airflow patterns, while drag and lift force coefficients quantify the forces exerted on the building by the wind. By quantifying and comparing these parameters for different design variations, engineers can assess the effectiveness of each design in mitigating wind loads and optimizing structural performance.

Analysing the influence of opening size, location, and orientation on wind loads and pressure fluctuations involves studying how these factors affect airflow patterns and pressure distributions around the building. The size of openings can significantly impact wind pressure, with larger openings potentially allowing more airflow through the building and reducing wind pressure on its surfaces. Similarly, the location and orientation of openings relative to prevailing wind directions can influence how effectively they mitigate wind loads. Engineers need to consider how different opening

configurations affect airflow dynamics, including potential wind tunnelling effects and pressure differentials between interior and exterior spaces. By analysing these factors, we can determine the optimal design parameters for openings that minimize wind loads while maintaining structural integrity and occupant comfort.

## **1.5 Outline of thesis**

The research work is explained in 5 chapters in this thesis.

**Chapter 1** provides a concise overview of the wind induced loads on tall building structures, outlining the objectives and scope of the current study.

**Chapter 2** provides an exhaustive review of existing literature and Research gap.

**Chapter 3** describes the model details and its validation by numerical simulation of investigating the wind effects on tall buildings using CFD

**Chapter 4** presents the Results & Discussion of these results for various cases.

**Chapter 5** encapsulated the conclusion and observations derived from this study and it also includes the scope of future research work.

# CHAPTER 2

## LITERATURE REVIEW

### 2.1 General

Wind load significance for tall buildings is paramount, as it directly impacts their structural integrity and safety. Due to their height and exposure, tall buildings face considerable wind forces that can cause swaying, vibrations, and structural stress. Properly analysing and addressing wind loads is crucial to prevent potential damage or failure, ensuring the building can withstand strong winds. This involves studying how wind interacts with the building's shape, orientation, and surface features to optimize its design. By effectively managing wind loads, engineers can enhance the stability, durability, and comfort of tall buildings, making them safer for occupants and more resilient against environmental challenges. Etc.

The purpose of this research is to determine the impact of wind on a tall building model with corner modifications and varying percentages of large openings, maintaining an equal area and consistent height across models. Wind effects are examined using numerical simulations in ANSYS CFX, with wind incidence angles ranging from 0 to 90 degrees. The numerical results are validated in this study and the external pressure coefficient ( $C_p$ ) results are compared with data from various experimental studies.

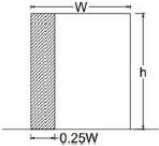
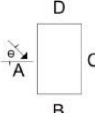
### 2.2 Indian Standards (IS 875:part-3:2015)

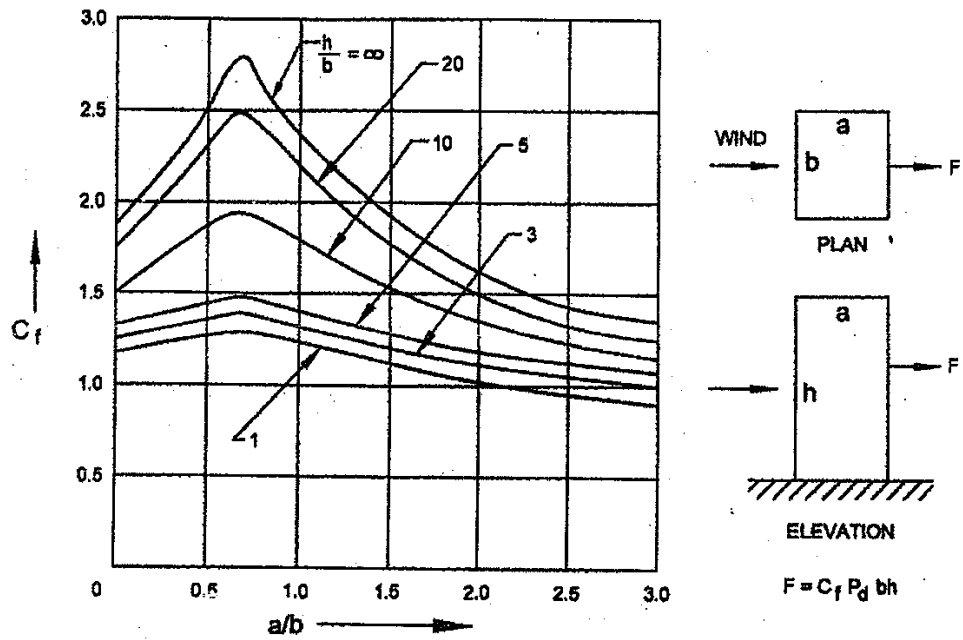
IS 875: Part 3: 2015 is an Indian Standard code that provides guidelines for the design loads, other than earthquake loads, for buildings and structures. Specifically, Part 3 of IS 875 deals with wind loads. This standard is crucial for architects, engineers, and builders as it outlines the methods to determine wind forces on structures to ensure their safety and stability.

The 2015 revision of IS 875: Part 3 includes updated procedures for calculating wind loads, taking into account factors such as wind speed, terrain, height, size, shape, and dynamic effects. It provides comprehensive information on how to account for wind loads during the design process, helping to mitigate the risks posed by strong winds and ensuring that buildings and structures can withstand wind forces over their expected lifetimes.

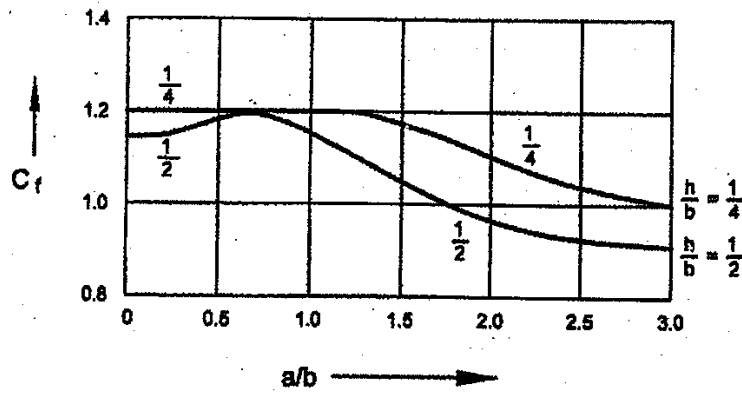
The present study utilizes Indian standards [2] to model wind speed, with the explanatory handbook [3] on these international standards providing a deeper understanding of wind behavior. As per IS 875:part-3:2015 Clause 6.3 specifies the design wind speed, while Table 5 (clause 7.3.3.1) discusses the external pressure coefficient for various building models. This data is used for numerical verification and validation of the study. The pressure coefficients for wind incidence angles of  $0^\circ$  and  $90^\circ$  for rectangular models are presented in tabular form. Additionally, the code includes force coefficients in clause 7.4.2.1, with typical values provided in Table 2.1, "Wind Pressure Coefficients on Rectangular Clad Buildings." Figure 2.1 illustrates the force coefficients for rectangular clad buildings in uniform flow [2] for isolated buildings.

**Table 2.1 Wind Pressure Coefficients on Rectangular Clad Building**  
**[Clause 7.3.3.1, IS 875(part-3,2015)]**

Building Height Ratio	Building Plan Ratio	Elevation	Plan	Wind Angle $\Theta$	C <sub>p</sub> for Surface				Local C <sub>pe</sub>
					A	B	C	D	
$\frac{3}{2} < \frac{h}{w} < 6$	$\frac{3}{2} \leq \frac{l}{w} < 4$			0	+0.7	-0.7	-0.4	-0.7	-1.2
				90	-0.5	-0.1	-0.5	+0.8	



a) Values of  $C_f$  versus  $a/b$  for  $h/b \geq 1$



b) Values of  $C_f$  versus  $a/b$  for  $h/b < 1$

**Fig. 2. 1** Force coefficient for rectangular clad buildings in uniform flow [2]

[(Clause 7.4.2.1, Fig. 4), IS: 875 (part-3); 2015]

## 2.3 Literature Review

- 2.3.1 Y. Li et al. [4]:** In this paper, the effects of building corner modifications on reducing wind loads on high-rise buildings with recessed, chamfered, and rounded corners is evaluated through pressure measurements in a boundary layer wind tunnel. The experiment revealed that chamfered corners significantly reduce along-wind loads at a wind direction of  $0^\circ$ , while recessed corners effectively reduce across-wind loads.
- 2.3.2 Fu-Bin Chen et al. [5]:** The author investigates the effects of incorporating openings in tall buildings through numerical simulations and wind tunnel tests. The findings indicate that adding openings to high-rise buildings significantly reduces the overall wind pressure coefficient, though it increases the mean wind pressure coefficient at specific local points. Placing openings in both the x-direction and y-direction can further decrease the mean and fluctuating wind pressure coefficients.
- 2.3.3 Ahmed Elshaer & Girma Bitsuamlak [6]:** In this optimization process, three strategically placed openings are introduced along the height of the building. These openings are designed to constitute 10% of the total building volume. This configuration aims to enhance the aerodynamic performance of the structure by allowing air to pass through, thereby reducing wind pressure and associated forces. As a result of these modifications, there is a significant reduction in the peak base moment coefficients. Specifically, the coefficients about the x-direction are reduced by 47%, and those about the y-direction by 42%. This substantial decrease in peak base moment coefficients indicates a notable improvement in the building's ability to withstand wind-induced forces, thereby enhancing its overall stability and structural integrity.

- 2.3.4 **N. Gaur and R. Raj [7]:** This paper explores the aerodynamic mitigation of wind loads on a square building model through corner modifications, using both Computational Fluid Dynamics (CFD) and wind tunnel experiments. It demonstrates that even minor modifications, such as cutting the corners of the building, can significantly reduce wind-induced drag force and moments by approximately 25% and 20%, respectively. The study finds that corner modifications are most effective when they alter 12–15% of the building's cross-sectional area, resulting in optimal aerodynamic performance. However, modifications exceeding 22% of the cross-section can compromise the structure's aerodynamic stability, potentially leading to instability under wind loads. This research underscores the importance of precise corner modification in improving the wind resistance of tall buildings without compromising their structural integrity.
- 2.3.5 **Paul and Dalui [8]** conducted a detailed numerical investigation aimed at understanding the influence of wind direction on the behaviour of a tall building featuring a distinctive "Z" plan shape. Their study uncovered noteworthy insights regarding the wind-induced effects experienced by different faces of the building. Specifically, their findings elucidate that the leeward face of the building encounters significant suction forces arising from frictional flow separations and the formation of vortices. These phenomena are vividly depicted through the observed streamlines, which distinctly illustrate the characteristics of flow separation and the presence of vortices in the vicinity of the building. Moreover, the combination of pressure exerted on the windward side and suction experienced on the leeward side results in the generation of vortices within the wake region, consequently leading to deflection of the building. Interestingly, the study also highlights that the windward face of the building is susceptible to suction forces due to flow separation occurring within the structure's limbs, alongside phenomena such as uplift, side wash, and backwash induced by the wind.



2.3.6 **Amin and Ahuja** [9] conducted a wind tunnel study at a reduced scale of 1:300, aiming to explore the mean interference effects between two rectangular buildings positioned in close proximity, featuring "L" and "T" plan shapes. The primary objective of the study was to scrutinize the distribution and intensity of wind pressure on the inner walls, with a particular focus on how these factors varied based on the arrangement of the building models, prevailing wind directions, and their relative dimensions. The observed variations stemmed from the interplay of wind flows influenced by the mutual interference induced by the presence of both building models.

2.3.7 **Pal and Raj** [10] conducted an experimental investigation into wind-induced pressure on square and fish-plan shapes under various interference conditions. The experiments were conducted in a 1:300 scale boundary layer wind tunnel with 100 percent obstruction between twin interfering models. The distance between the twin building models was set at 10% of the building model's height. The study revealed that the average pressure coefficient ( $C_p$ ) values of the fish-plan shape building model differ significantly from those of the square and rectangular plan shape building models. Therefore, relying solely on structural and cladding design investigations from regular plan shape buildings under identical working conditions may not be adequate. This is particularly relevant due to the unique cross-sectional plan shape of the fish-plan building model, which results in high turbulence at certain faces under all interference conditions. This turbulence is notably pronounced as the cross-sectional plan of the fish-plan shape building model is gradually increased and then decreased, distinguishing it from the square plan shape building model and other interference studies.

- 2.3.8 **Chakraborty et al.** [11] conducted experimental investigations on wind effects using wind tunnel testing. They observed that changes in wind direction could result in varying pressures on different surfaces of a building shaped like a "plus" sign. Depending on the surface's location, the pressure may either increase or decrease. Symmetrical faces experience identical pressure distributions due to the symmetrical nature of wind flow at different wind angles.
- 2.3.9 **Sheng et al.** [12] conducted experiments using a wind tunnel at a scale of 1:300 on a high-rise building to examine pressure loads under atmospheric boundary layer flow. Their study revealed that inlet conditions have a significant impact on velocity and turbulent intensity profiles. The front face consistently experiences upstream flow effects, while the lateral faces are subject to vortex shedding. Additionally, wind behaviour varies depending on ground conditions.
- 2.3.10 **Mooneghi and Kargarmoakhar** [13] conducted a review focusing on reducing wind loads through shape optimization. They emphasized that architectural drawings often dictate the shape of a building, prompting the need for aerodynamic modifications to mitigate wind effects. These modifications aim to disrupt flow streamlines around the building model or alter flow patterns in the downstream wind. By employing various methods, such as altering the external shape of the building, it is possible to change flow patterns downstream of the wind. This, in turn, reduces the wake effect in the downstream wind direction, ultimately minimizing the impact of wind on the structure.

2.3.11 **Bandi et al.** [14] conducted experimental research on the aerodynamic characteristics of six high-rise building models in a boundary layer wind tunnel. Their study revealed that the mean wind force values were higher for triangular models compared to square section models. Additionally, they found significant variations in the local wind force coefficients of the 1800 helical and 3600 helical models with height. These variations contributed to reducing the total wind force coefficient for the helical models.

2.3.12 **Merrick and Bitsuamlak** [15] investigated the shape effect on the wind induced response of high-rise building of various shape like square, circular, triangular, rectangular and elliptical. Some shapes are highly prone to adverse wind effects such as vortex shedding which can generate the high dynamic load which controls the design parameters. Elliptical, triangular and rectangular shaped buildings were found highly susceptible to high torsion loading.

2.3.13 **Kawai** [16] conducted a wind tunnel test to explore corner modifications on tall buildings, investigating variations such as corner cuts, recessions, and roundness. The study found that incorporating rounded corners effectively enhances aerodynamic damping, thereby mitigating instability. Tall buildings with square or rectangular sections are particularly prone to aeroelastic instabilities in turbulent boundary layer flow. This susceptibility arises because the approaching flow separates from the windward corner, generating strong vortices through the roll-up of the separated shear layer. Modifying the windward corner proves highly effective in reducing drag and lift by altering flow patterns, which impacts various flow characteristics such as reattachment and narrows the wake width downstream of the wind. Interestingly, the study revealed that the suppression of aeroelastic instability resulting from small corner cuts and recessions is not due to the inhibition of vortex shedding, but rather stems from increased aerodynamic damping.

**2.3.14 Irwin [17]** conducted experimental assessments of wind effects on bluff bodies and determined that the flow around these bodies is attributed to the formation of robust vortices in their wakes. This phenomenon significantly influences the impact of wind on tall buildings. By modifying the corner shape of a building model, it's possible to reduce the base moment and base shear at the building's base by up to 25%. Additionally, incorporating openings can diminish the negative pressure in the wake region to a considerable extent, resulting in substantial savings in the structure due to reduced wind loads in both drag and crosswind directions.

**2.3.15 Miyashita et al. [18]** conducted a study to evaluate the wind-induced response of tall buildings with square shapes and chamfered corners using wind tunnel testing. They found that wind-induced vibrations could be mitigated by altering the building's corners and incorporating effective openings in the model. Comparatively, models with corner cuts or openings exhibited smaller across-wind fluctuating wind force coefficients than those with a square plan shape, particularly at a wind incidence angle of  $0^\circ$ . Additionally, when analysing the combined displacement values obtained from wind force correlation, it was observed that they were larger than the combined value of the maximum value plus standard deviation, especially at a wind incidence angle of  $10^\circ$ .

**2.3.16 Bhattacharya et al. [19]** examined the pressure distribution on different faces of tall buildings with an "E" plan shape under wind loads through both experimental and numerical studies. Their findings revealed variations in pressure compared to square plan-shaped models. The highest positive pressure of 0.8 was recorded under  $180^\circ$  wind, while the most substantial negative pressure of -0.68 occurred during  $90^\circ$  wind. It's noted that numerical results could differ based on meshing properties and sizes. The distribution of pressure significantly hinges on the plan shape of these tall buildings.

**2.3.17 Bhattacharyya and Dalui [20]** conducted both experimental and numerical analyses on a tall building shaped like the letter "E." They observed that symmetrical faces of the building exhibited identical pressure distribution patterns. The error between numerical simulation and experimental results fell within acceptable limits. They proposed a general equation for pressure distribution specific to each face of the "E" shaped model. Similar pressure distributions were noted on corresponding faces for two different wind incidence angles. However, a change in flow pattern was observed at wind incidence angles of 30° and 120°. This altered flow pattern directly impacted pressure variations in the wake region of the building.

**2.3.18 Zaki et al. [21]** conducted a wind tunnel experiment on a single-zone building equipped with a wind catcher on two sides and a window. They measured mean and fluctuating surface pressures to examine how turbulent flows affect building ventilation. The study highlights that the building's exterior plays a substantial role in influencing inlet flow through the rooftop wind catcher openings. Additionally, the presence of a window is crucial for optimizing flow rates when using wind catchers.

**2.3.19 Kwok [22]** conducted a wind tunnel experiment to explore the impact of wind on tall buildings with a rectangular cross-sectional shape. The study revealed that incorporating horizontal slots, slotted corners, and chamfered corners led to a notable reduction in both along-wind and across-wind responses. When the incident wind struck the wide face of the building, the cross-wind force spectra exhibited a prominent peak at a critical location. Conversely, when the wind was perpendicular to the narrow face of the building, the peak in the cross-wind force spectra was broader and less distinct. Remarkably, buildings with chamfered corners showed an absence of this peak. The modified building shapes were tested and demonstrated a considerable reduction in the magnitude of cross-wind excitation forces.

**2.3.20 Stathopoulos [23]** conducted an experimental investigation of ground-level wind conditions around buildings with chamfered corners using a boundary layer wind tunnel. The experiment involved testing two shapes of tall buildings: one with a square corner and another with a chamfered corner, with variations in the model's height. It was observed that chamfering the corner at a 45-degree angle resulted in a notable reduction in the size of the strong wind area in the corner region. However, the chamfered corner had minimal impact on turbulence conditions in the corner region. Instead, it influenced flow separation and decreased turbulence on the windward face of the building. Additionally, as the building's height increased, wind velocities and the size of the strong wind area in the corner stream increased for both square and chamfered buildings, while turbulence conditions remained relatively unaffected.

**2.3.21 Raj and Ahuja [24]** conducted wind tunnel tests in an open-circuit boundary to explore the impact of wind loads on tall buildings with cross-sectional shapes, varying them while maintaining equal floor areas. They found that a building experiences maximum wind load when it presents the maximum exposed area to direct wind incidence. The shape of the building's cross-section significantly influences the wind loads it encounters, with an increase in these forces observed compared to a square section, reflecting the impact of the building's cross-sectional shape. Additionally, wind loads vary with changes in wind incidence angles.

2.3.22 **Verma et al. [25]** conducted experimental research to examine the impact of wind on tall square buildings with varying wind incidence angles. They observed that, for most wind incidence angles, positive pressure increased with height. Additionally, for wind incidence angles at 0 degrees, negative pressure increased from the windward edge to the leeward edge. Notably, the average pressure coefficients ( $C_p$ ) on the building faces and the pressure distribution on these faces differed significantly from values specified in international standards.

2.3.23 **Sharma et al. [26]** conducted a comprehensive review on strategies to mitigate wind loads on tall buildings through various modifications. Techniques such as chamfering, rounding, recession, and incorporating slotted corners have been shown to effectively reduce wake turbulence by up to 30%. The alteration of flow structure depends on both the type and extent of modification, as different modifications can impact flow patterns differently. Additionally, variations in cross-sectional shape at mid-height can also modify flow patterns. For instance, the upper region of an octagonal plan-shaped cross-section has been observed to reduce wake turbulence compared to a square plan-shaped cross-section. Tall structures with bluff shapes are particularly susceptible to wind-induced vibrations, but these effects can be mitigated through structural or aerodynamic adjustments.

2.3.24 **Bandi et al. [27]** examined the peak pressure exerted on tall buildings across various configurations. Among the models tested, which included shapes such as triangular, square, pentagon, hexagon, octagon, dodecagon, circular, and clover, the combination of helical and corner cuts demonstrated the most significant reduction in  $C_{p \text{ max}}$ . Specifically, the model with a tri-corner cut exhibited a smaller maximum negative peak pressure coefficient compared to the triangular model. However, the model with square corner cuts displayed a larger maximum negative peak pressure coefficient than the square model.

**2.3.25 Goyal et al. [28]** examined the impact of wind loads on a tall building shaped like the letter "Y" using Computational Fluid Dynamics (CFD). They observed that at the edge of the windward side, the wind velocity reaches its maximum, while it is lowest on the leeward side. After implementing corner modifications, they noted that the rounded corner on the windward side experienced the highest wind speed. In the case of a spherical model, the smaller size of the eddy contributed to greater stability. Direct wind flow resulted in a positive pressure distribution on the windward face, while flow separation and vortex generation led to a negative pressure distribution on the leeward face.

**2.3.26 Sanyal and Dalui [29]** conducted a numerical investigation into the impacts of courtyards and openings on a tall building with a rectangular floor plan under wind load, utilizing ANSYS CFX. They observed that the windward surface of the model, which is directly exposed to the wind, experiences consistent wind forces, resulting in positive pressure coefficients. Conversely, the leeward and side faces of the building encounter suction pressure due to frictional flow separation and the generation of vortices. The formation of vortices in the wake zone occurs when there is a combination of windward side pressure forces and leeward side suction forces, causing the structure to deflect.

**2.3.27 Keerthana and Harikrishna [30]** examined the impact of wind on rectangular and "H" section structures using Computational Fluid Dynamics (CFD). The study compared the results obtained from CFD simulations with those from wind tunnel experiments, revealing a closer alignment between the two sets of results. However, deviations between numerical and experimental results were observed in mean lift coefficients, particularly as the angle of wind incidence varied. While windward pressure coefficients were accurately predicted for both turbulence models, some disparities were noted in the wake region downstream of the wind.



## 2.4 Research Gap

It is observed from above studies that for the wind induced load reduction corner modification is mainly provided. Sometimes provision for large opening also is provided but their combination for wind induced load reduction is not available for various type of tall building. However, there is a lack of research examining the combined effect of corner modification and large openings for various types of tall buildings. This study addresses this gap by analyzing wind pressure on a square-shaped tall building, considering both corner modification and large openings. Computational Fluid Dynamics (CFD) simulations in ANSYS Workbench are conducted on 1:100 scale models to assess the combined impact. Corner modification involves recessed and chamfered corners, along with large openings occupying 10%, 20%, and 30% of the frontal area. The study evaluates the aerodynamic mean pressure coefficient ( $C_p$ ) and pressure distribution across different faces of the building models, comparing results to identify the model with the lowest wind load.

# **CHAPTER 3**

## **METHODOLOGY**

### **3.1 General**

As previously outlined in Chapter 1, the primary objective of this study is to analyse wind pressure on a square-shaped building model, considering the combined impact of corner modification and large openings, through Computational Fluid Dynamics (CFD). This chapter details the methodology employed to investigate wind effects on tall building models using numerical simulations.

### **3.2 Numerical Simulations**

In this study, numerical simulation is carried out using boundary conditions similar to those employed by Revuz et al. [31] and Frank et al. [32]. It is essential that the simulation results are validated against previous experimental results or international standards. The simulation domain is established based on recommendations from various numerical investigations. The simulations, conducted using ANSYS CFX, utilize the k- $\epsilon$  turbulence model.

#### **3.2.1 Computational Fluid Dynamics (CFD)**

Computational Fluid Dynamics (CFD) is a branch of engineering that focuses on solving fluid dynamics equations using the finite element method. This technique involves breaking down a fluid domain into smaller elements, creating various meshing patterns, and then solving numerical equations for each element. These meshing patterns collectively simulate the behaviour of fluids within the entire domain.

At the core of fluid dynamics problems in CFD are the Navier-Stokes equations, which are based on three fundamental conservation laws: conservation of mass, conservation of momentum, and conservation of energy. These equations describe how fluids move and interact, providing a comprehensive framework for analysing fluid behaviour in complex engineering systems.

### 3.3 Modelling

The investigation of wind effects on high-rise structures can be conducted using two methods: wind tunnel testing and Computational Fluid Dynamics (CFD). Wind loads are evaluated using the formulas provided in the IS: 875 (part-3): 2015 [2].

Design wind speed

$$V_z = V_b K_1 K_2 K_3 K_4 \quad \dots\dots\dots(3.1)$$

Where;

$V_b$  = Basic wind speed;

$K_1$  = Probability factor;

$K_2$  = Terrain, height and structure size factor;

$K_3$  = Topography factor and

$K_4$  = Importance factor for cyclonic region.

Design wind pressure

$$P_z = 0.6 \times V_z^2 \quad \dots\dots\dots(3.2)$$

Where;

$P_z$  = Wind pressure at height Z, in N/m<sup>2</sup>

$V_z$  = Design wind speed at height Z in m/s

$$P_d = K_d K_a K_c P_z \quad \dots\dots\dots(3)$$

Where;

$K_d$  = Wind directionality factor;

$K_a$  = Area averaging factor and

$K_c$  = Combination factor.

The value of  $P_z$  shall not be taken less than  $0.70 P_z$

Force and pressure method

$$F = (C_{pe} - C_{pi}) A P_d \quad \dots\dots\dots(4)$$

Where;

$F$  = Wind force

$C_{pe}$  = External pressure coefficient

$C_{pi}$  = Internal pressure coefficient

$A$  = Effective area of structure

$P_d$  = Design wind pressure

$$F = C_f A P_d \quad \dots\dots\dots(5)$$

Where;

$F$  = Wind force

$C_f$  = Force coefficient

$A$  = Effective area of structure

$P_d$  = Design wind pressure

### 3.4 Model Details

In this study, the Models of scale 1:100 length scale is used for the analysis. The models with square corners, recessed corners and chamfered corners with opening of 0%, 10%, 20% and 30% are analysed using CFD simulations in ANSYS WORKBENCH. These models have identical length, width and height which is 200mmx200mmx600mm and the openings are provided in two parts of equal area.

The pressure coefficients variation around the different faces of these tall buildings is discussed in this study. Plan cross sectional shape of models with variation in the corner configuration is presented in Figure.3.1. In this figure, Model A shows the square shape building model without any corner modification, Model B shows the Recessed corners modification and Model C shows the Chamfered corners modification. For the modification of both corners, an equal size of 10 mm is used. With the corner modifications, openings of three different percentages are also provided in two equal parts along the height of the building.

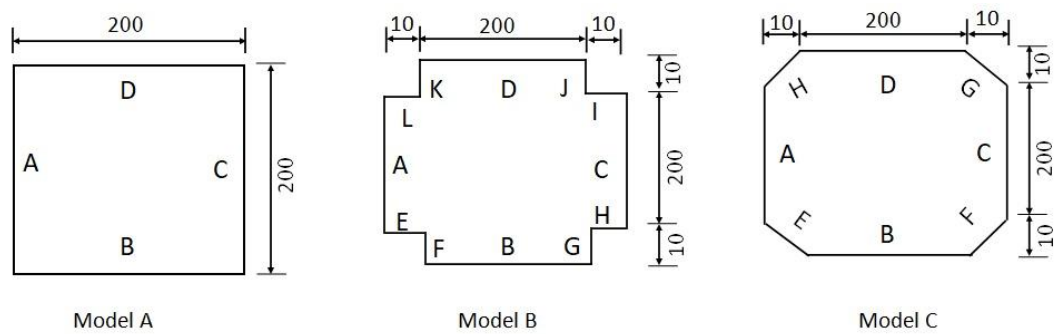


**Fig. 3. 1** Plan View of Models with various Corner Modifications

Isometric view is for the model-A, model-B, and model-C is illustrated in the Figure.3.2.

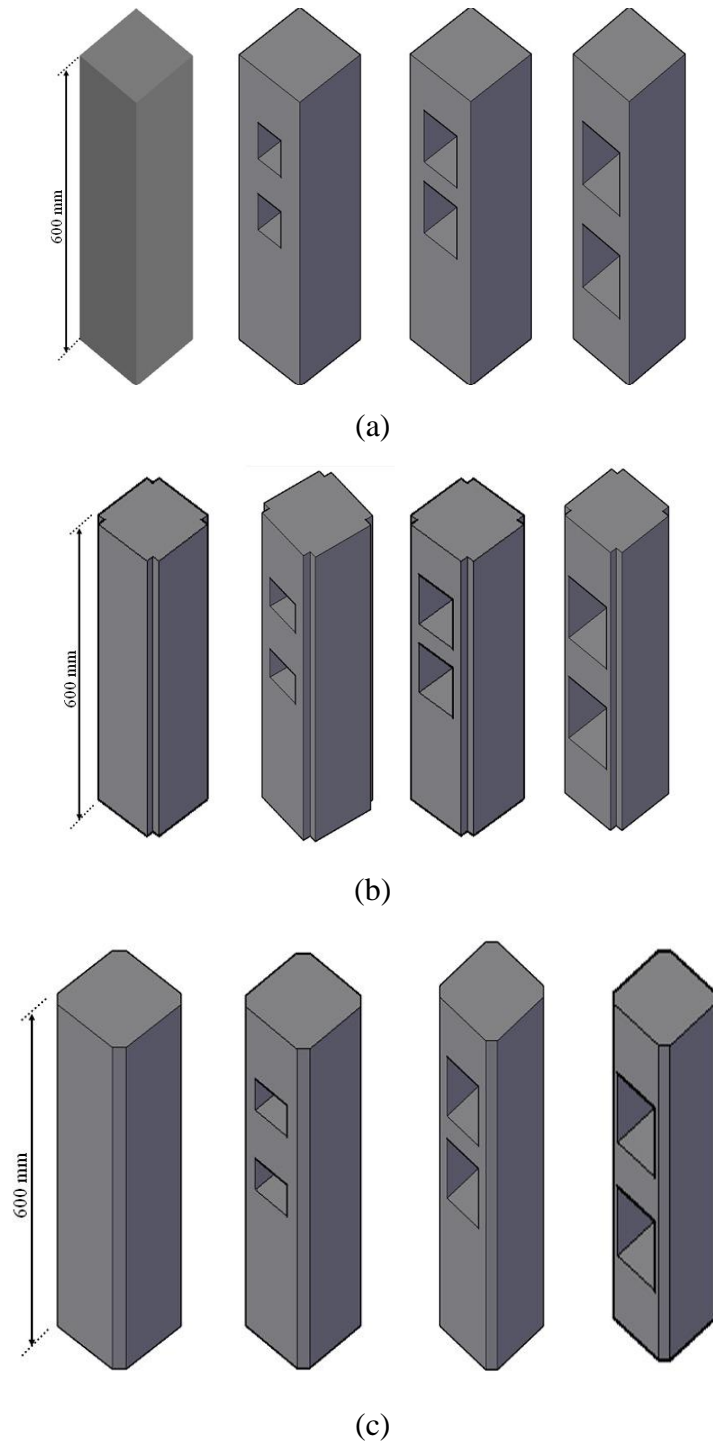


**Fig. 3. 2** Isometric view of Model A, B and C

The primary objective of this study was to compare the wind-induced effects on various tall building models, as previous studies for wind induced load reduction have largely concentrated on either on the corner modification or on the provision of large openings. The present study not only studied the corner modification building model alongside with provision of large openings.

### 3.5 Boundary Conditions

Using the CFD simulations, the impact of wind on building models is investigated. In order for CFD to function, an area is divided into the grid with many cells. The grid of cells is then initialized, encircled by boundaries that replicate the surfaces, opened and closed spaces, boundary pressure, and air movements inside the cell. In order for simulation to develop the flow effectively, as advised by Revuz et al. [31] and Frank et al. [32], the inlet, top, and sidewall borders are taken into consideration  $5H$  from the model, while the outlet boundary is positioned at  $15H$  behind the model. The domain with the top and side walls remaining free slip condition in the CFX configuration setup is shown in Figure 3.3. In this study, the ground and building model surfaces are regarded as no-slip walls in the context of CFX configuration setup. The definition of no-slip is "when the air velocity at the wall boundary equals the air velocity at the domain inlet". The definition of free slip is "shear stress and velocities normal to the wall are both set to zero, while velocity components parallel to the wall have a finite value". The free stream velocity at the inlet of domain considered to be as  $10\text{ m/s}$ .

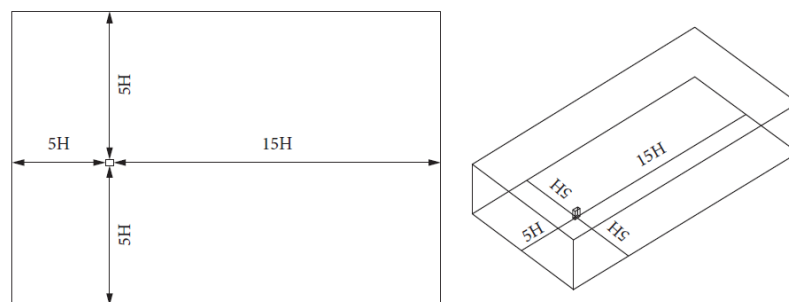


**Fig. 3. 3** Domain used in CFD Simulation

### 3.6 Meshing

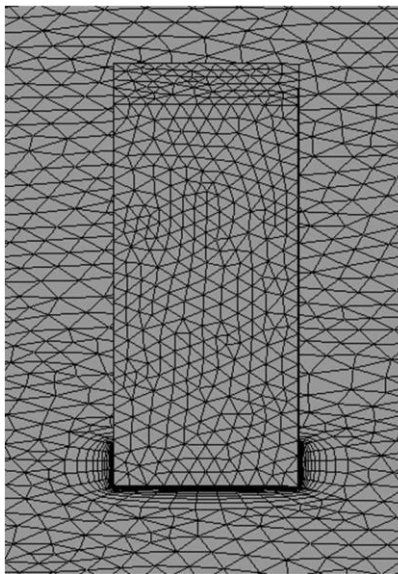
Meshing must be carefully designed to effectively solve numerical problems, and various CFD tools are available for this purpose. Meshing captures important flow features, which depend on flow parameters such as grid refinement within the wall boundary layer. The meshing process begins with drawing the geometry as required. Once the geometry is created in a design modular or any other tool, it can be imported into the design modular. The named selection of the geometry is very important to help CFX-Pre understand the building model's configuration and define flow physics. It is best to named selection before meshing so that the surface mesh aligns precisely with the nodes on both sides of the boundary, ensuring a more accurate fluid solution. The named selection also aids the program in controlling inflation, which will automatically be applied to walls during auto mesh generation.

The mesh generation steps are automated within the program, but users can retain control over the process by modifying the element size, mesh type, and refinement sites. There are other kinds of meshing; for models that are directly imported with clean CAD geometry, ANSYS provides tetra dominant meshing, which usually uses bigger mesh sizes. For CAD models with several surface patches, the patch-independent tetra dominant meshing method works well. This type of meshing is also suitable for geometries with small edges.

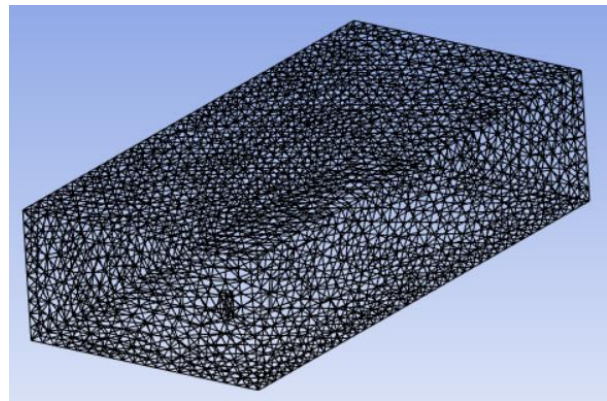
Inflation is applied to accurately capture the flow at the interface, using various methods available in CFD. The standard approach, smooth transition, is a popular technique that computes each local height and total height for a smooth rate of volume change using the size of the local tetrahedron element. The starting height of each inflated triangle is determined by averaging its area at the nodes. The starting heights of a uniform mesh and a variable mesh will be different and comparable, respectively. The overall height of the inflation layers decreases as the growth rate value increases. The asymptotic value in relation to the number of inflation layers is the total height of



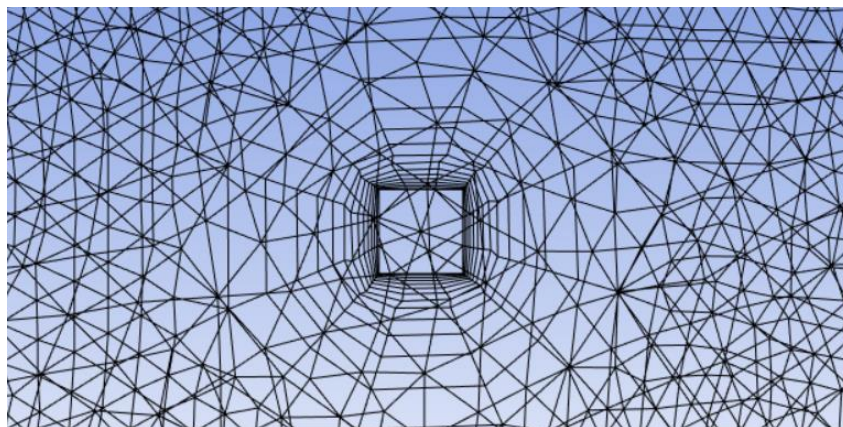
these layers. In order to reach the specified maximum thickness, the total thickness option uses growth rate and layer count settings to produce layers that are constantly inflated. The first layer thickness option generates constant inflation layers using the first layer height, maximum layers, and growth rate to control the inflation mesh. done in the numerical simulation by ANSYS CFX is shown in Figure 3.4.



(a)



(b)



(c)

**Fig. 3. 4** Different types of Meshing(a) Building Meshing (b) Domain Meshing  
(c) Inflation

### 3.7 Validation

Validation is performed on the square building model which do not have any type of corner modification nor any large openings. Validation is pre-requisite of the numerical simulation for these purposes square model is selected because the data already available to validate. The main objective of this study was the investigation of wind effect on model with different corner configurations and large openings. The coefficient of pressure obtain from this validation is compared with values given in **Clause 7.3.3.1, IS 875 (part-3,2015) [2]**. This is clearly shown as the numerical simulation results yield nearly identical values for the pressure coefficient. Additionally, the results from this CFD study have been compared with those from other available CFD and experimental studies.

# CHAPTER 4

## RESULTS AND DISCUSSION

### 4.1 General

Due to limited land availability, tall buildings are very common. Structural engineers need to design these buildings to minimize the impact of wind. With the rapid global population growth, the demand for high-rise projects is increasing. These projects, including skyscrapers and tall towers, require careful evaluation against wind effects, which influence structural parameters like shape and openings. Wind effects can be investigated using various techniques such as wind tunnel tests and computational fluid dynamics tools. In this study we obtained our results by using computational fluid dynamics (CFD) in ANSYS CFX.

Regularly shaped structures are very common in tall buildings. However, in recent decades, due to land use constraints, the use of regular shapes has been declining. Consequently, buildings with irregular shapes are now being constructed worldwide. This research focuses on a square building with a cross-sectional area of 40,000 m<sup>2</sup> and a height of 60 meters. The study examines wind incidence angles ranging from 0° to 90°.

### 4.2 Pressure contours

Pressure contours in Computational Fluid Dynamics (CFD) represent the distribution of pressure on the surfaces within the flow field being analyzed. These contours are visualized as lines or color gradients on a plot, where each line or color indicates a

constant pressure value. By examining these contours, engineers and researchers can gain insights into how pressure varies across different regions of a fluid flow, such as around an object or within a boundary layer. Pressure contours help identify high and low-pressure areas, which are crucial for understanding aerodynamic forces, optimizing design, and ensuring structural integrity in various applications, including aerospace, automotive, and civil engineering.

The pressure on the front face (Face A) i.e. windward face is positive and negative on the back face (Face C) i.e. leeward face for Model A, Model B and Model C as shown in Figure 4.1, Figure 4.2 and Figure 4.3 respectively. The Pressure contours for Model A with opening of 0%, 10%, 20% & 30% in which Face A has max. pressure in the center, then it decreasing towards the corner region. The other faces of Model A have negative pressure as shown in Figure 4.1. The Face B & Face D (Side Faces) have pressure reducing in the direction of the wind Movement. In case of openings, the maximum pressure is just above the top opening at the front Face A and the side faces i.e. Face B and Face D shows similar pressure distribution as the 0% opening Model. The leeward face i.e. Face C have negative pressure increase in between the two opening as the size of opening increases.

In Model B and C due to corner modifications the pressure is significantly reduces on the front Face A and the maximum positive pressure exist only in smaller region at the center and on the side faces (Face B and Face D) shows similar pressure distribution as Model A where pressure is reducing in the direction of the wind Movement. In Model B, the Recessed faces (Face E, F, G, H, I, J, K & L) pressure distribution is positive on Face E & Face L and negative on all others faces. In Model C, the Chamfered faces (Face E, F, G & H) pressure distribution is positive on Face E & Face H and negative on Face F & Face G because these faces are in the leeward wind direction as shown in Figure 4.2 and Figure 4.3. All of these pressure contours obtained from ANSYS CFX analysis.

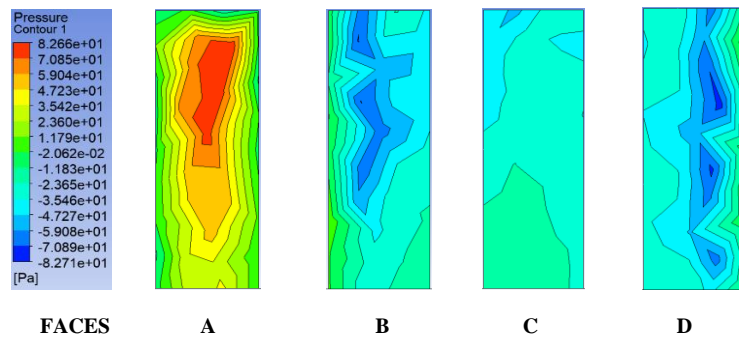


**Figure 4.1.1 Pressure counters for 0% Opening**

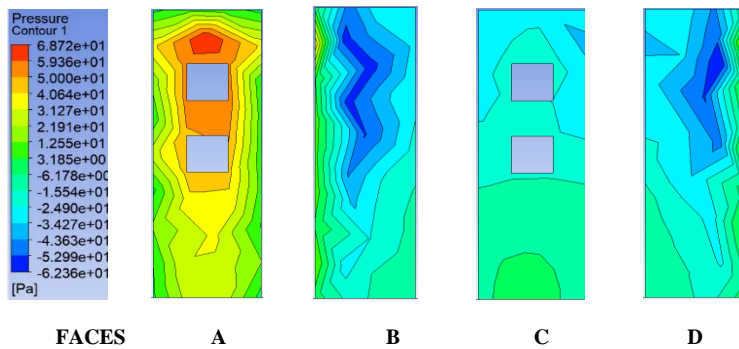


**Figure 4.1.2 Pressure counters for 10% Opening**

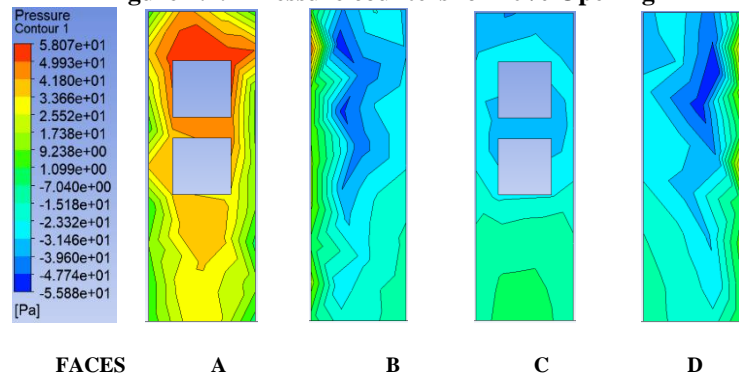


**Figure 4.1.3 Pressure counters for 20% Opening**

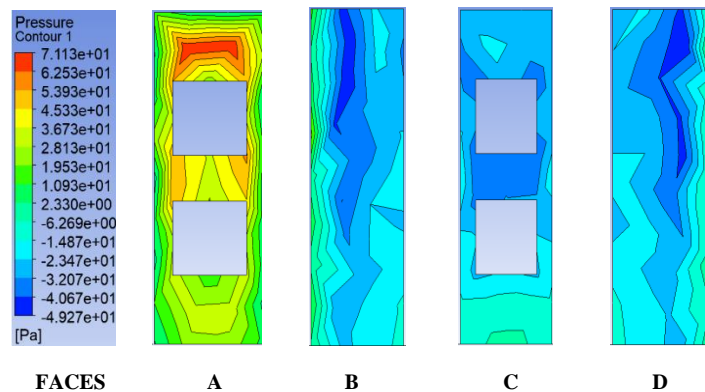


**Figure 4.1.4 Pressure counters for 30% Opening**

**Fig. 4. 1 Pressure contours at different percentage of openings of Model A**

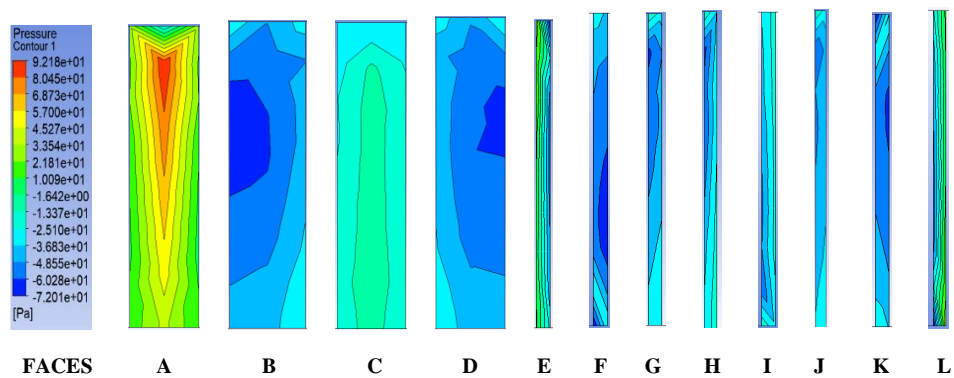


Figure 4.2.1 Pressure counters for 0% Opening

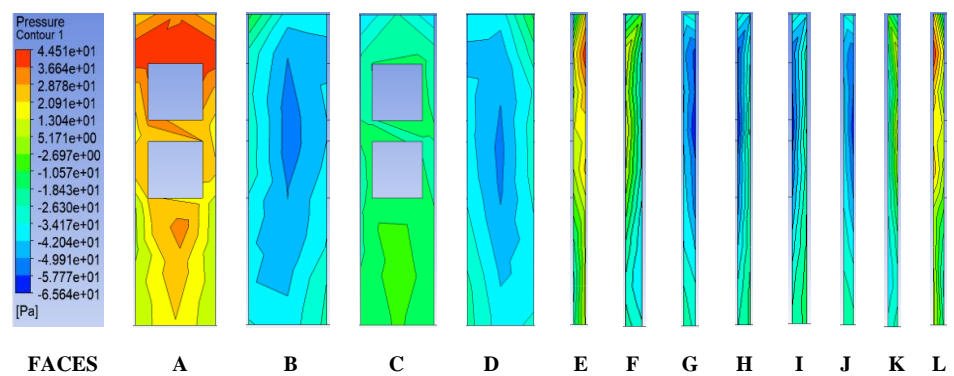


Figure 4.2.2 Pressure counters for 10% Opening

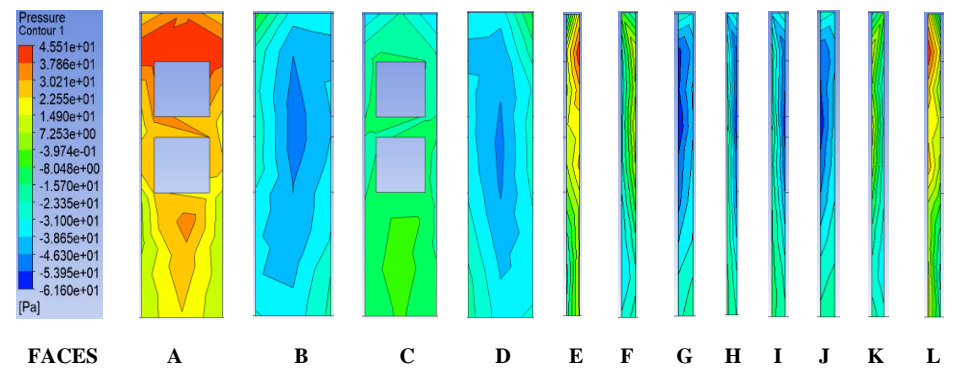


Figure 4.2.3 Pressure counters for 20% Opening

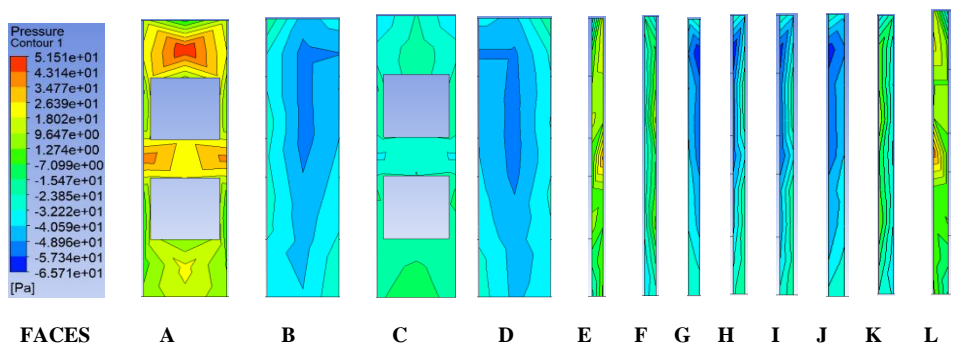


Figure 4.2.4 Pressure counters for 20% Opening

Fig. 4. 2 Pressure contours at different percentage of openings of Model B

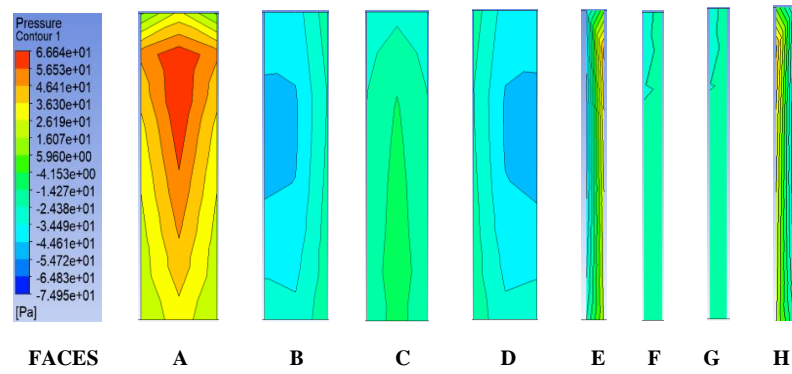


Figure 4.3.1 Pressure counters for 0% Opening

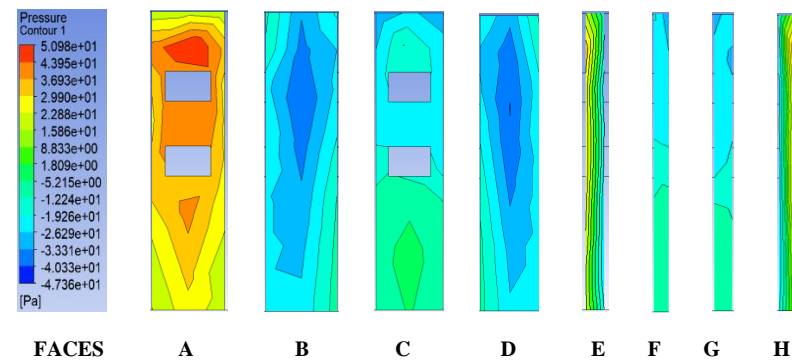


Figure 4.3.2 Pressure counters for 10% Opening

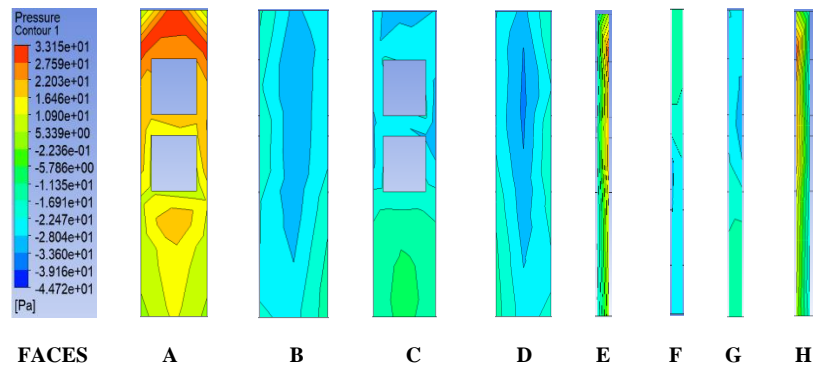


Figure 4.3.3 Pressure counters for 20% Opening

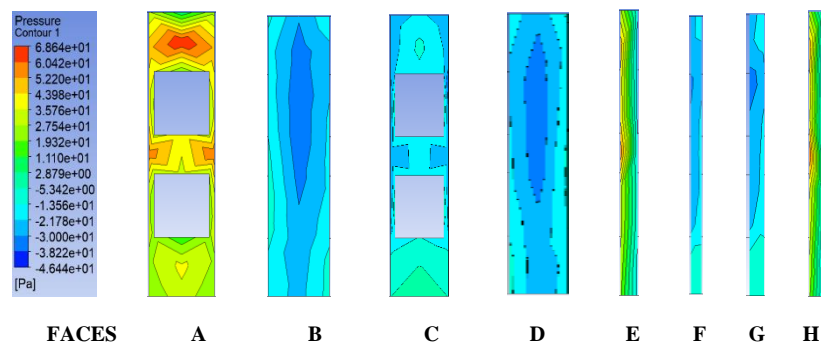


Figure 4.3.4 Pressure counters for 30% Opening

Fig. 4.3 Pressure contours at different percentage of openings of Model C



### 4.3 Velocity streamlines

Streamlines are hypothetical path lines which represent the trajectories taken by fluid particles within a fluid flow, providing insight into the directional movement of fluid elements at any given point in the flow field in the CFD model. Figure 4.4, Figure 4.5 and Figure 4.6 display the streamline patterns for Model A, Model B, and Model C at a wind incidence angle of  $0^\circ$  under various Percentage of Opening conditions. Due to the modifications made to the building corners and large openings, distinct flow patterns are seen for each of the three models. In building models with 0% openings, vortices are generated across their entire height. As the result of this, the building models' leeward side is being subjected to negative pressure.

As the size of opening is increases the size of vortices is reducing on leeward side of the building model. In comparison to the Model A and Model C the vortices are less in Model B due the corner modifications the recessed corner model producing less vortex as compare to the Models with the square and chamfered corners as shown in the Figure 4.4, Figure 4.5 and Figure 4.6.

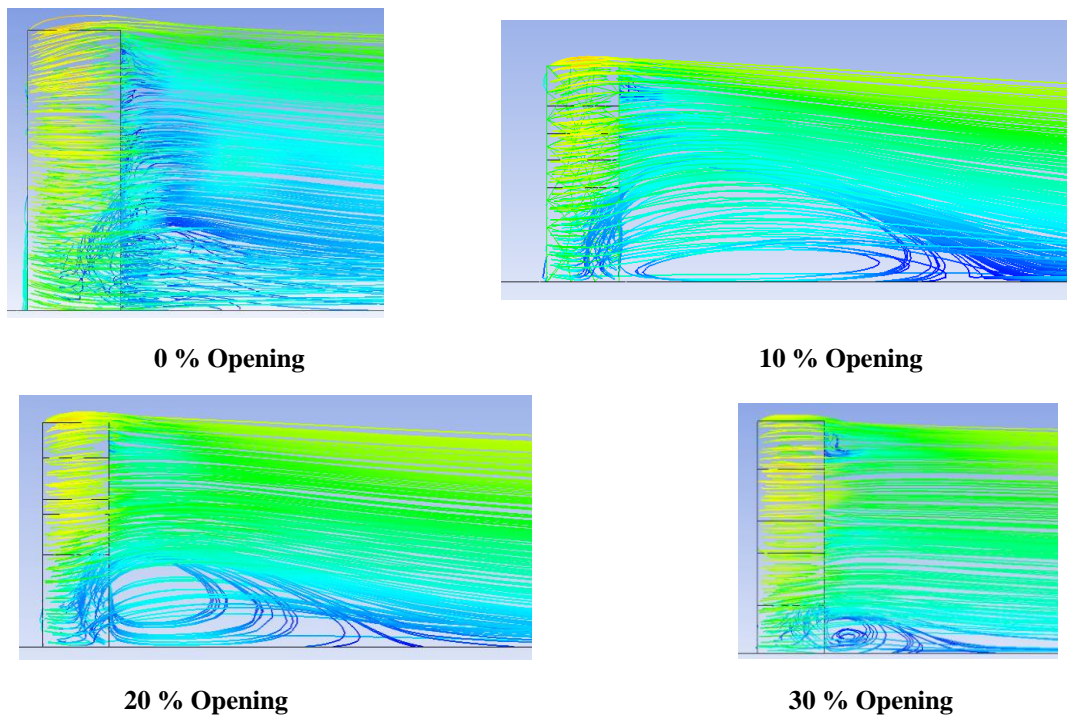
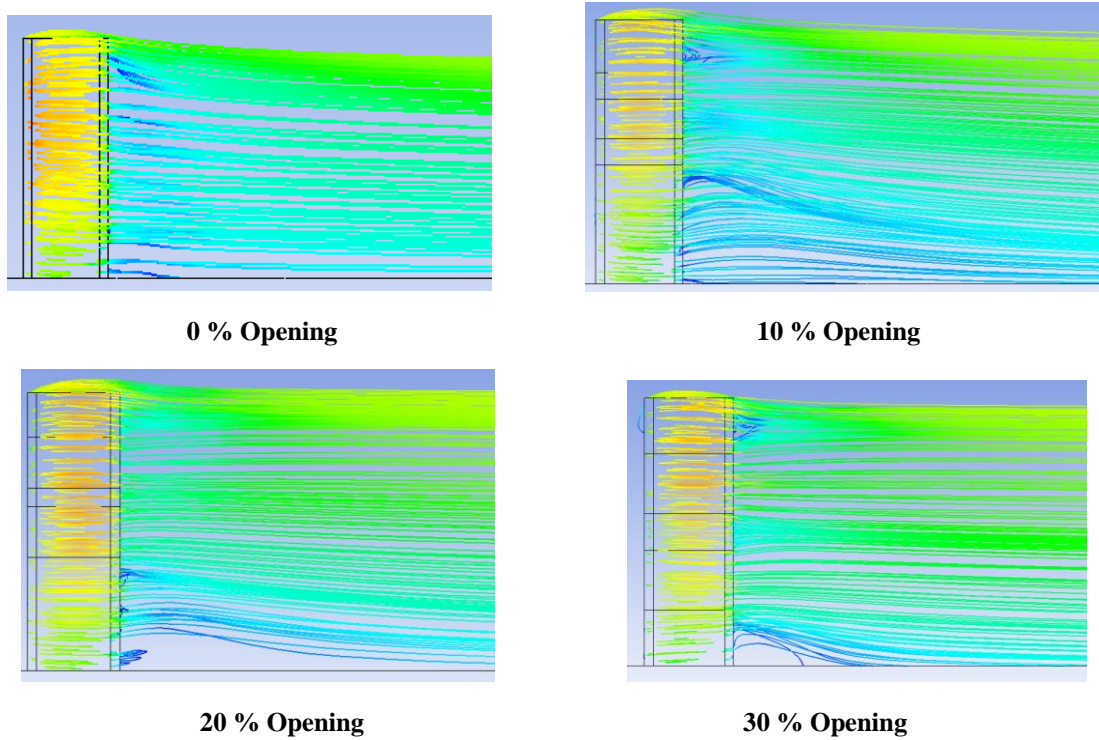
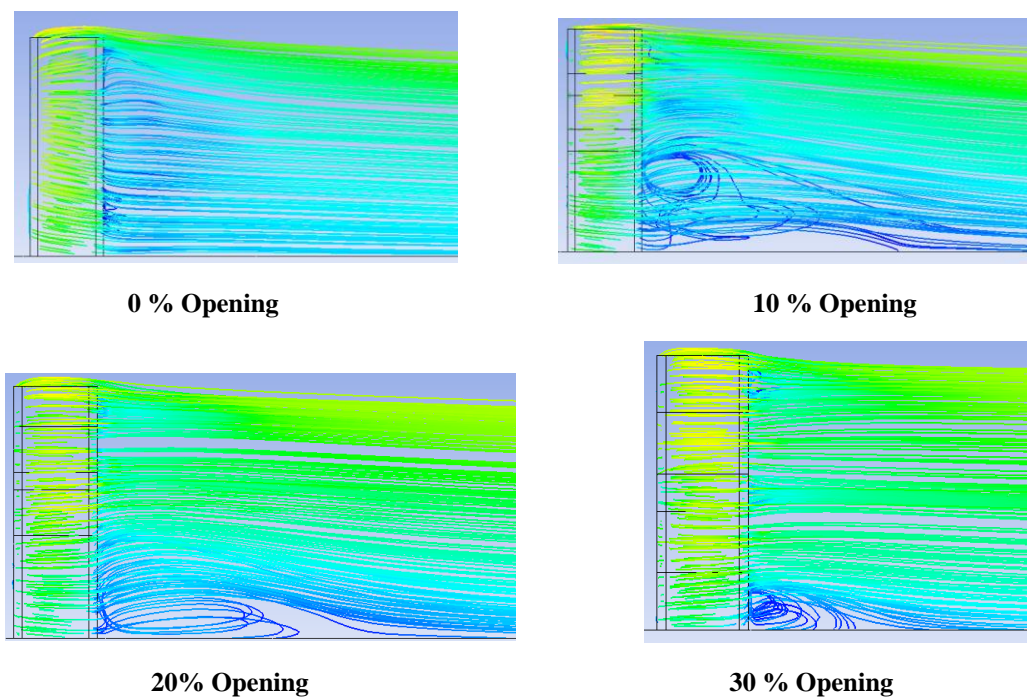


Fig. 4. 4 Streamlines for Model A for different opening conditions





**Fig. 4. 5** Streamlines for Model B for different opening conditions



**Fig. 4. 6** Streamlines for Model C for different opening conditions

#### 4.4 Coefficient of Pressure (C<sub>p</sub>)

The coefficient of pressure (C<sub>p</sub>) in Computational Fluid Dynamics (CFD) is a dimensionless number that describes the relative pressure distribution over the surface of an object immersed in a fluid flow. It is defined as the difference between the local static pressure on the surface and the free-stream static pressure, normalized by the dynamic pressure of the free-stream flow. The coefficient of pressure is essential for analysing aerodynamic and hydrodynamic performance, as it provides insights into the pressure forces acting on the surface, which are crucial for understanding lift, drag, and overall stability.

C<sub>p</sub> is crucial in CFD because it provides a normalized measure of pressure distribution, allowing for comparison across different surfaces and flow conditions. A C<sub>p</sub> value of 1 indicates a pressure higher than the free-stream pressure, typically found in stagnation points where the fluid velocity is nearly zero. A C<sub>p</sub> value of 0 corresponds to the free-stream pressure, and negative C<sub>p</sub> values indicate lower pressures, which often occur in regions of accelerated flow. Understanding C<sub>p</sub> is essential for aerodynamic and hydrodynamic analyses. In summary, the coefficient of pressure (C<sub>p</sub>) in CFD is a fundamental parameter that encapsulates pressure variations on surfaces within a flow field, providing critical insights for optimizing and understanding fluid dynamics in engineering applications.

The mean pressure coefficient (C<sub>p</sub>) is calculated from equation (4.1) given below, where  $p$  is the pressure which has been measured from the required point,  $p_o$  is the reference height of steady pressure,  $\rho$  is density of the air which is taken as 1.225 [kg/m<sup>3</sup>] and  $U_H^2$  refers to the mean wind velocity at the building reference heights.[1]

$$C_{Pmean} = \frac{P - P_o}{\frac{1}{2}\rho U_H^2} \quad \text{----- Equation (4.1)}$$

The highest value of coefficient of pressure ( $C_p$ ) is acting on windward face i.e. Face A of Model C for 0% opening condition with value 0.769898 and lowest value of coefficient of pressure ( $C_p$ ) is acting on Model B with 0 % opening condition on leeward face i.e. Face B of value -0.86652.

The graph different values of Coefficient of pressure ( $C_p$ ) for all three Models with different opening conditions are given below in Table 4.1, Table 4.2 and Table 4.3.

**Table 4. 1 Coefficient of pressure ( $C_p$ ) for Model A for different % of Opening conditions**

	Coefficient of pressure ( $C_p$ )			
	Face A	Face B	Face C	Face D
Opening %				
0%	0.5948101	-0.508322	-0.3792333	-0.4794318
10%	0.4616718	-0.4616718	-0.419904	-0.4249528
20%	0.3713887	-0.3987507	-0.4372232	-0.4258168
30%	0.4885949	-0.4557022	-0.4383517	-0.4482612

**Table 4. 2 Coefficient of pressure ( $C_p$ ) for Model B for different % of Opening conditions**

	Coefficient of pressure ( $C_p$ )			
	Face A	Face B	Face C	Face D
Opening %				
0%	0.69429	-0.86652	-0.31222	-0.83575
10%	0.549055	-0.58653	-0.38167	-0.6545
20%	0.441949	-0.64519	-0.32806	-0.63357
30%	0.515832	-0.68228	-0.37032	-0.56846

**Table 4. 3 Coefficient of pressure ( $C_p$ ) for Model C for different % of Opening conditions**

	Coefficient of pressure ( $C_p$ )			
	Face A	Face B	Face C	Face D
Opening %				
0%	0.7698984	-.0.73241	-0.3207203	-0.7287262
10%	0.6005976	-0.5714762	-0.3869192	-0.5497332
20%	0.4740323	-0.4500147	-0.4118733	-0.5571742
30%	0.6060852	-0.437519	-0.4375464	-0.5306664

The graph showing different value of Coefficient of pressure ( $C_p$ ) for all three Models with different opening conditions are given below

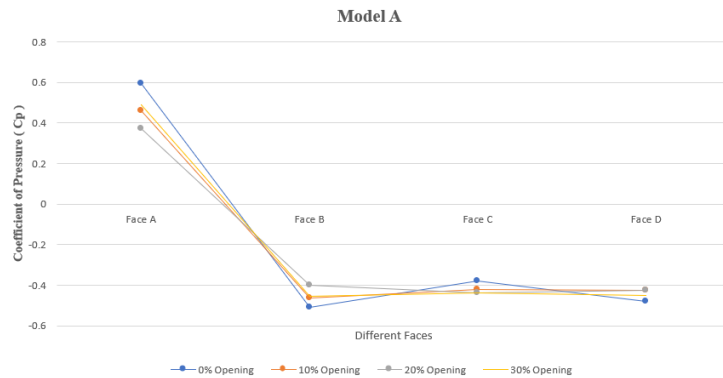


**Fig. 4. 7** Coefficient of pressure ( $C_p$ ) for Model A for different % of Opening conditions

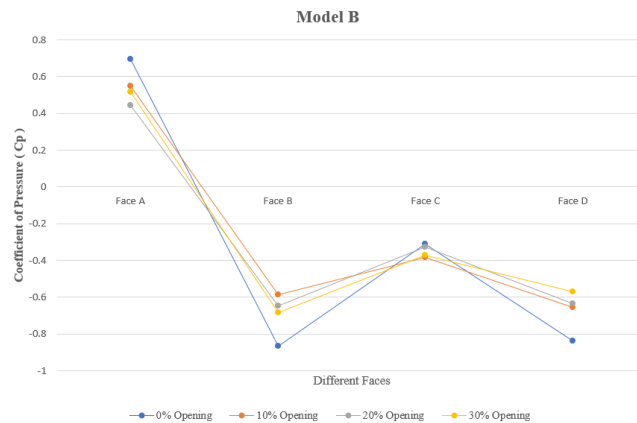


**Fig. 4. 8** Coefficient of pressure ( $C_p$ ) for Model A for different % of Opening conditions

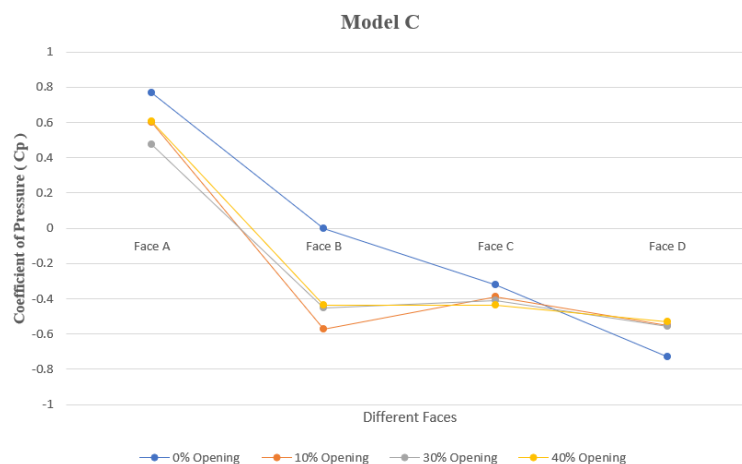


**Fig. 4. 9** Coefficient of pressure ( $C_p$ ) for Model A for different % of Opening conditions

#### 4.5 Drag Force Coefficients ( $C_{fx}$ & $C_{fy}$ )

In Computational Fluid Dynamics (CFD), the Drag Force Coefficients, denoted as ( $C_{fx}$  &  $C_{fy}$ ), are critical parameters used to quantify the resistance experienced by an object moving through a fluid.  $C_{fx}$  refers to the drag force coefficient in the direction of the flow (typically the x-direction), while  $C_{fy}$  represents the drag force coefficient perpendicular to the flow direction (typically the y-direction). These coefficients are dimensionless numbers that encapsulate the effects of shape, surface roughness, and flow conditions on the drag force. They are calculated by normalizing the drag force by the product of the fluid density, the square of the flow velocity, and a reference area. Understanding these coefficients is essential for optimizing designs in engineering applications such as automotive, aerospace, and civil engineering, where minimizing drag can lead to improved performance and efficiency.

For an extended duration of a period of time wind engineers are researching wind load. Quantifying the effects of wind on structures proves challenging due to the complex nature of structural geometry and the variability of field conditions. This study derives force coefficients in the X-direction ( $C_{fx}$ ) and Y-direction ( $C_{fy}$ ) through equations (4.2) and (4.3).

$$C_{fx} = \frac{F_x}{(0.5\rho U_h^2 \cdot A_p)} \quad \text{----- Equation (4.2)}$$

$$C_{fy} = \frac{F_y}{(0.5\rho U_h^2 \cdot A_p)} \quad \text{-----Equation (4.3)}$$

Where as  $\rho$  represents the air density,  $U_h$  denotes the velocity referenced at the height of the building model and  $A_p$  signifies the projected area in the wind direction. [1]

For  $0^\circ$  incidence angle highest coefficient of drag in X-direction ( $C_{fx}$ ) is acting on Model A and Model C with 0% opening condition on windward face i.e. Face A of value 1.6364 and 1.64108 respectively. The lowest value of  $C_{fx}$  is acting on Model B with 30% opening condition with the value of .7858. The highest Drag coefficient in Y-direction ( $C_{fy}$ ) is acting on Model A with 30 % opening condition with value of .006348 and the lowest value of  $C_{fy}$  is -0.0002489 which is obtain from Model A with 0% opening condition on windward Faces. The different values of Coefficient of Drag in X-direction ( $C_{fx}$ ) for various % of openings with incidence angle of  $0^\circ$  an which are shown in figure 4.10.

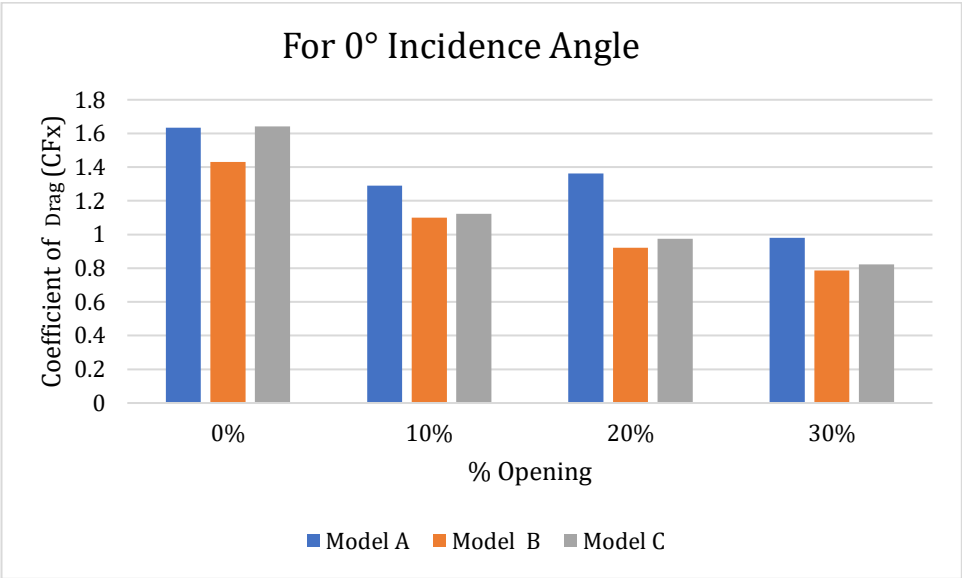


**Fig. 4. 10** Coefficient of Drag in X-direction ( $C_{fx}$ ) for  $0^\circ$  incidence angle

For 30° incidence angle highest coefficient of drag in X-direction ( $C_{fx}$ ) is acting on Model A with 0% opening condition on windward face i.e. Face A of value 1.788. The lowest value of  $C_{fx}$  is acting on Model B with 30% opening condition with the value of .5568. The highest Drag coefficient in Y-direction ( $C_{fy}$ ) is acting on Model A with 20 % opening condition with value of .006642215 and the lowest value of  $C_{fy}$  is 0.0000351983 which is obtain from Model B with 0% opening condition on windward Faces. The different values of Coefficient of Drag in X-direction ( $C_{fx}$ ) for various % of openings with incidence angle of 30° which are shown below in and figure 4.11.

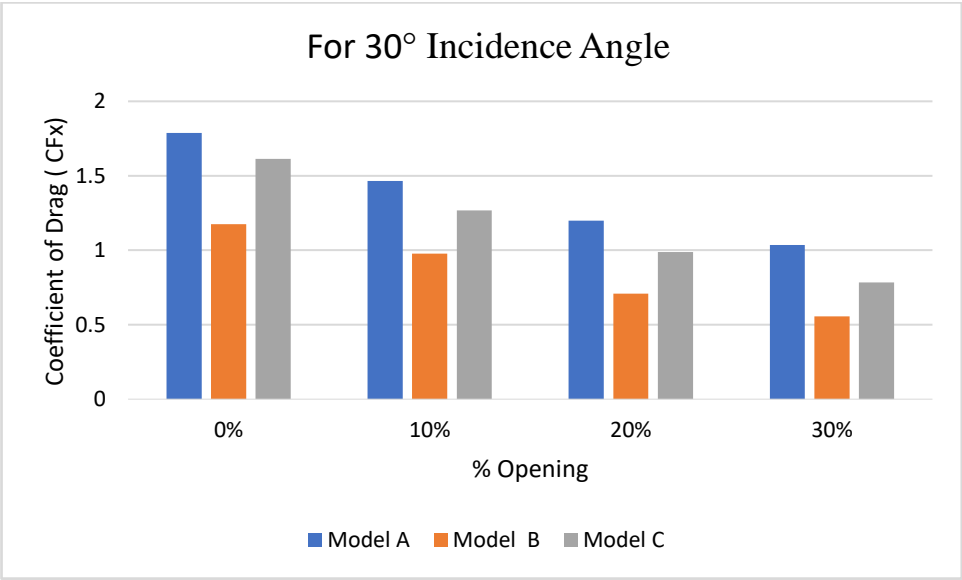


**Fig. 4. 11** Coefficient of Drag in X-direction ( $C_{fx}$ ) for 30° incidence angle



# CHAPTER 5

## Conclusions

### 5.1 Summary

The main objective of this study is to compare and analysis of tall building models for wind-induced load reduction providing corner modification with provision large openings of different sizes. In this study, the research has been conducted on horizontal and vertical aerodynamic treatments to mitigate wind effects on tall buildings, there remains a lack of research on the combined effects of corner modifications and large openings along the height of buildings for reducing wind loads on tall structures.

### 5.2 Conclusion

The following conclusion is obtained after analyzing different Models by numerical simulation in ANSYS CFX and comparing their results.

- a) By providing 10 % and 20 % openings in Building model leads to the reduction of coefficient of pressure ( $C_p$ ) about 20 to 25 % on the windward faces.
- b) In Corner Modification, Recessed corner Modification is leading to the approx. 13 % reduction in Coefficient of Drag in X-direction ( $C_{fx}$ ) and introduction of opening with corner modification also helps in Coefficient of Drag in X-direction ( $C_{fx}$ ) reduction by a significant amount.
- c) Drag force reductions can possibly be a consequence of suction around the corner cut in the walls, as indicated by the streamline analysis and the pressure field of the models.

## References

1. Meena, R.K., Raj, R. and AnbuKumar, S., 2022. Numerical investigation of wind load on side ratio of high-rise buildings. In *Advances in Construction Materials and Sustainable Environment: Select Proceedings of ICCME 2020* (pp. 937-951). Springer Singapore.
2. IS: 875 (2015), Indian Standard design loads (other than earthquake) for buildings and structures-code of practice, part 3(wind loads) 2015.
3. S. 64 (S&T) 2001, “Explanatory Handbook on Indian Standard Code of practice for design loads (other than earthquake) For buildings and structures, Part 3 Wind Loads (IS 875 (PART 3): 1987,” New Delhi Bur. Indian Stand. New Delhi 110002, 2001., pp. 1238–1241, 1995.
4. Li, Y., Tian, X., Tee, K.F., Li, Q.S. and Li, Y.G., 2018. Aerodynamic treatments for reduction of wind loads on high-rise buildings. *Journal of Wind Engineering and Industrial Aerodynamics*, 172, pp.107-115.
5. Chen, F.B., Wang, X.L., Zhao, Y., Li, Y.B., Li, Q.S., Xiang, P. and Li, Y., 2020. Study of Wind Loads and Wind Speed Amplifications on High-Rise Building with Opening by Numerical Simulation and Wind Tunnel Test. *Advances in Civil Engineering*, 2020(1), p.8850688.
6. Elshaer, A. and Bitsuamlak, G., 2018. Mult objective aerodynamic optimization of tall building openings for wind-induced load reduction. *Journal of Structural Engineering*, 144(10), p.04018198.
7. Gaur, N. and Raj, R., 2022. Aerodynamic mitigation by corner modification on square model under wind loads employing CFD and wind tunnel. *Ain Shams Engineering Journal*, 13(1), p.101521.

8. R. Paul and S. K. Dalui, "Wind effects on 'Z' plan-shaped tall building: a case study," *Int. J. Adv. Struct. Eng.*, vol. 8, no. 3, pp. 319–335, 2016.
9. J. A. Amin and A. Ahuja, "Wind-induced mean interference effects between two closed spaced buildings," *KSCE J. Civ. Eng.*, vol. 16, no. 1, pp. 119–131, 2012.
10. S. Pal and R. Raj, "Evaluation of Wind Induced Interference Effects on Shape Remodelled Tall Buildings," *Arab. J. Sci. Eng.*, no. 0123456789, 2021.
11. S. Chakraborty, S. K. Dalui, and A. K. Ahuja, "Experimental investigation of surface pressure on '+' plan shape tall building," *Jordan J. Civ. Eng.*, vol. 8, no. 3, pp. 251–262, 2014.
12. R. Sheng, L. Perret, I. Calmet, F. Demouge, and J. Guilhot, "Wind tunnel study of wind effects on a high-rise building at a scale of 1:300," *J. Wind Eng. Ind. Aerodyn.*, vol. 174, no. September 2017, pp. 391–403, 2018.
13. M. Asghari Mooneghi and R. Kargarmoakhar, "Aerodynamic Mitigation and Shape Optimization of Buildings: Review," *J. Build. Eng.*, vol. 6, pp. 225–235, 2016.
14. E. K. Bandi, Y. Tamura, A. Yoshida, Y. Chul Kim, and Q. Yang, "Experimental investigation on aerodynamic characteristics of various triangular-section high-rise buildings," *J. Wind Eng. Ind. Aerodyn.*, vol. 122, pp. 60–68, 2013.
15. R. Merrick and G. Bitsuamlak, "Shape Effects on the Wind-Induced Response of High-Rise Buildings," *J. Wind Eng.*, vol. 6, no. 2, pp. 1–18, 2009.
16. H. Kawai, "Effect of corner modifications on aeroelastic instabilities of tall buildings," *J. Wind Eng. Ind. Aerodyn.*, vol. 74–76, pp. 719–729, 1998.

17. P. A. Irwin, "Bluff body aerodynamics in wind engineering," *J. Wind Eng. Ind. Aerodyn.*, vol. 96, no. 6–7, pp. 701–712, 2008.
18. K. Miyashita et al., "Wind-induced response of high-rise buildings Effects of corner cuts or openings in square buildings," *J. Wind Eng. Ind. Aerodyn.*, vol. 50, no. C, pp. 319–328, 1993.
19. B. Bhattacharyya, S. K. Dalui, and A. K. Ahuja, "Wind induced pressure on 'E' plan shaped tall buildings," *Jordan J. Civ. Eng.*, vol. 8, no. 2, pp. 120–134, 2014.
20. B. Bhattacharyya and S. K. Dalui, "Investigation of mean wind pressures on 'E' plan shaped tall building," *Wind Struct. An Int. J.*, vol. 26, no. 2, pp. 99–114, 2018.
21. A. Zaki, P. Richards, and R. Sharma, "The effect of onset turbulent flows on ventilation with a two-sided rooftop windcatcher," *J. Wind Eng. Ind. Aerodyn.*, vol. 225, no. December 2021.
22. K. C. S. Kwok, "Effect of building shape on wind-induced response of tall building," *J. Wind Eng. Ind. Aerodyn.*, vol. 28, no. 1–3, pp. 381–390, 1988.
23. T. Stathopoulos, "Wind environmental conditions around tall buildings with chamfered corners," *J. Wind Eng. Ind. Aerodyn.*, vol. 21, no. 1, pp. 71–87, 1985.
24. R. Raj and A. K. Ahuja, "Wind Loads on Cross Shape Tall Buildings," *J. Acad. Ind. Res.*, vol. 2, no. 2, pp. 111–113, 2013.
25. S. k. Verma, A. K. Ahuja, and A. D. Padey, "Effects of wind incidence angle on wind pressure distribution," *J. Acadmia Ind. Res.*, vol. 1, no. May, pp. 747–752, 2013.

26. A. Sharma, H. Mittal, and A. Gairola, "Mitigation of wind load on tall buildings through aerodynamic modifications: Review," *J. Build. Eng.*, vol. 18, no. September 2017, pp. 180–194, 2018.
27. E. K. Bandi, H. Tanaka, Y. C. Kim, K. Ohtake, A. Yoshida, and Y. Tamura, "Peak Pressures Acting on Tall Buildings with Various Configurations," *Int. J. High-Rise Build.*, vol. 2, no. 3, pp. 229–244, 2013.
28. P. K. Goyal, S. Kumari, S. Singh, R. K. Saroj, R. K. Meena, and R. Raj, "Numerical Study of Wind Loads on Y Plan-Shaped Tall Building Using CFD", *Civ. Eng. J.*, vol. 8, no. 02, pp. 263–277, 2022.
29. P. Sanyal and S. K. Dalui, "Effects of courtyard and opening on a rectangular plan shaped tall building under wind load," *Int. J. Adv. Struct. Eng.*, vol. 10, no. 2, pp. 169–188, 2018.
30. M. Keerthana and P. Harikrishna, "Application of CFD for assessment of galloping stability of rectangular and H-sections," *J. Sci. Ind. Res. (India)*, vol. 72, no. 7, pp. 419–427, 2013.
31. Revuz, J., Hargreaves, D.M. and Owen, J.S., 2012. On the domain size for the steady-state CFD modelling of a tall building. *Wind and structures*, 15(4), p.313.
32. Franke, J., Hellsten, A., Schlünzen, H. and Carissimo, B., 2010, May. The Best Practise Guideline for the CFD simulation of flows in the urban environment: an outcome of COST 732. In *The Fifth International Symposium on Computational Wind Engineering (CWE2010)* (pp. 1-10).

## SCOPUS INDEXED CONFERENCE

Meena, M., Sharma, D. and Raj, R. (2024) “Study of tall buildings for wind induced load reduction by providing recessed corner with large openings” International Conference on Civil, Environment and Construction Technology: Ecological Resilient & Sustainable Development Goals Integration – Research Agenda (CECT-2024), Department of Civil Engineering, Graphic Era (Deemed to be) University, Dehradun, 17<sup>th</sup>-18<sup>th</sup> May 2024.



PAPER NAME

Complete Thesis - Copy.docx

WORD COUNT

9051 Words

CHARACTER COUNT

50565 Characters

PAGE COUNT

48 Pages

FILE SIZE

3.4MB

SUBMISSION DATE

May 30, 2024 12:29 PM GMT+5:30

REPORT DATE

May 30, 2024 12:30 PM GMT+5:30

● 6% Overall Similarity

The combined total of all matches, including overlapping sources, for each database.

- 4% Internet database
- Crossref database
- 3% Submitted Works database
- 3% Publications database
- Crossref Posted Content database

● Excluded from Similarity Report

- Bibliographic material
- Cited material
- Quoted material
- Small Matches (Less than 12 words)

Head, Deptt. of Civil Engineering  
Delhi Technological University  
Govt. of NCT of Delhi  
(Formerly Delhi College of Engg.)  
Shabbad Daulatpur, Bawana Road  
Delhi-110042